


## Article

# Utilization of Basalt Dust as Waste Material in Cement Grouts for Geothermal Application

Krzysztof Seńczuk <sup>1</sup>, Aneta Sapińska-Śliwa <sup>2,\*</sup>  and Tomasz Kowalski <sup>2</sup>

<sup>1</sup> Doctoral School, AGH University of Science and Technology in Krakow, Adama Mickiewicza 30 Avenue, 30-059 Kraków, Poland

<sup>2</sup> Laboratory of Geoenergetics, AGH University of Science and Technology in Krakow, al. Adama Mickiewicza 30, 30-059 Kraków, Poland

\* Correspondence: ans@agh.edu.pl; Tel.: +48-12-617-2217

**Abstract:** Research on the utilization of the Earth's heat focuses mainly on effective sourcing of energy accumulated in rock mass. One of the most important parameters is thermal conductivity, which can be modified using various compositions of cement grouts. Hardened cement slurry is intended to improve thermal conductivity. It should function as a sort of extension of the rock mass to the outer diameter of heat exchanger tubes. Regardless of the thermal conductivity of the rock, high conductivity of the grout increases the energy efficiency of the BHE. Heat accumulated in the rock mass can be extracted using borehole heat exchangers (BHE), in which high thermal conductivity of cement slurry is wanted over the entire length of the exchanger. Generally, in case of deep borehole heat exchangers (DBHE), it is recommended to use two types of cement slurry, one with reduced thermal conductivity in the upper part of the exchanger and grout with increased thermal conductivity in its lower part. When cementing geothermal wells, cement grout with decreased thermal conductivity along the entire length of the borehole is most commonly used. Geothermal boreholes extract geothermal water which, at the surface, is used for heating, for example. Then, after use, the cooled water is injected through injection holes. In this article, two different basalt dusts are examined. These dusts were obtained by crushing basalt boulders in open-pit mines. They were examined for their effect on thermal conductivity when added to grout. According to the Polish Ordinance of the Minister of Environment dated 9 December 2014 regarding the waste catalogue, they were classified as waste. The materials, named basalt dust A and basalt dust B, were used to create cement slurries with a water–cement ratio of 0.5–0.7 with a wide range of percentage concentration of basalt dust. The test results show that as concentrations in the slurry increase, the values of thermal conductivity and strength decrease. This correlation occurred for both tested additives.

**Keywords:** cement slurry; basalt dust; thermal conductivity; borehole heat exchangers; geothermal wells; hardened grout; flexural strength; compressive strength



**Citation:** Seńczuk, K.; Sapińska-Śliwa, A.; Kowalski, T. Utilization of Basalt Dust as Waste Material in Cement Grouts for Geothermal Application. *Energies* **2022**, *15*, 7033. <https://doi.org/10.3390/en15197033>

Academic Editors: Abdul-Ghani Olabi, Zhien Zhang and Michele Dassisti

Received: 15 July 2022

Accepted: 21 September 2022

Published: 25 September 2022

**Publisher's Note:** MDPI stays neutral with regard to jurisdictional claims in published maps and institutional affiliations.



**Copyright:** © 2022 by the authors. Licensee MDPI, Basel, Switzerland. This article is an open access article distributed under the terms and conditions of the Creative Commons Attribution (CC BY) license (<https://creativecommons.org/licenses/by/4.0/>).

## 1. Introduction

There is an increasing amount of research focusing on the most efficient use of energy stored in the rock mass. For now, Earth's heat is extracted by means of three basic types of boreholes: boreholes heat exchangers (BHE), deep borehole heat exchangers (DBHE), and geothermal wells. There is no specified depth boundary which determines when we can assign a borehole as BHE or DBHE, according to its length. Some authors determine that borehole heat exchangers have depth up to 500 m [1]. Based on the available geothermal resources and on the requested energy needs for heating and cooling buildings, BHEs can usually reach 200 m in depth [2]. For the purpose of this article, we assumed that a borehole heat exchanger has depth up to 200 m, as it reflects commonly installed lengths of BHE in Poland. When drilling BHEs, DBHEs and geothermal wells, it is important to use cement grout suitable for a given type of borehole. In BHEs, it is recommended to use cement

grout with increased thermal conductivity over the entire length of the exchanger [3–5]. However, in case of DBHEs two types of cement slurry should be used: one that reduces thermal conductivity near the surface to reduce the escape of heat into the ground and one that increases thermal conductivity in deeper areas to maximize heat collection from the Earth. In a DBHE, it may be that the temperature of the heat carrier entering the exchanger from the surface will be higher than the temperature of the rock mass; then, this carrier in the upper part of the DBHE will cool down. This is not advantageous; therefore insulation of the upper part of the DBHE should be used. One of the possibilities is to use grout with reduced thermal conductivity. At the later stage of circulation (flow of the carrier in the annular space of the DBHE towards the bottom), the temperature of the upper body increases, which causes a change in the direction of the heat flow. This phenomenon is then beneficial and should be intensified by increasing the thermal conductivity of the cement slurry. Geothermal wells should be cemented with low thermal conductivity grout along the entire length in order to minimize heat losses as much as possible [6,7]. In Poland, heat losses are significant due to a considerable depth of wells, most of which substantially exceed 1500 m. For example, a large geothermal installation located in Podhale (southern Poland), has several geothermal wells cemented with traditional cement used in oil wells. One of the boreholes has a capacity of 550 m<sup>3</sup>/h. If cement slurry with reduced thermal conductivity were used for this borehole, an increase of 4–5 °C in outflow temperature would be achieved, and thus an annual energy gain would be obtained. It would increase from 2.49 to 3.11 MW. Similar calculations are also submitted in the literature [8].

Research on thermal conductivity of cement grouts used for borehole heat exchangers has been performed by many scientists. Most frequently checked and described are additives which increase the thermal conductivity of grout. Currently tested additives that increase thermal conductivity include:

- Expanded natural graphite (ENG) [9,10];
- Graphene nanoplatelets (GNPs) [11];
- Randomly distributed graphite nanosheets (R-GNs) and oriented graphite nanosheets (O-GNs) [12];
- Graphite [13–15];
- Magnesium flakes [16];
- Reduced graphene oxide [17];
- Graphene [18,19].

Research has also been conducted on reducing the thermal conductivity of cement slurries. However, this has not been on such scale as in the case of additives increasing thermal conductivity. The following additives were examined:

- Hydroxyethylcellulose [20];
- Magnetite powder [21];
- Dolomite drill cuttings [22].

Nowadays, due to increased popularity of heat pumps in Europe, e.g., in Poland, research on increasing or decreasing heat conductivity value of cement grouts seems to be important. In September 2021 in Poland, 15 new concessions for exploration and recognition of geothermal waters and development of hydrogeological documentation were granted. Considering an average depth of geothermal well which ranges from 1.5 to 3 km, thermal energy losses can be significant without the use of properly selected grout. Energy losses affect directly installation operational costs. Therefore, it is important to find and do research on the materials that reduce boreholes' thermal conductivity. They will increase their energy efficiency of extracting heat from water.

Waste utilization will reduce the world's waste accumulation. One of the solutions is to use it as an additive to sealing grouts. That is why research to check their applicability is important. For the purposes of this article, two of these kinds of materials were examined. They were examined for their effects on the thermal conductivity and strength of cement slurries. This is one of the first, if not the first study of this kind conducted on basalt

dust. Basalt dust can be safely applied to soils. Crushed basalt rocks such as basalt flour are used, e.g., as a fertilizer for flowers, shrubs, trees, vegetables and fruits. Given that a waste producer has to pay for its disposal, it is highly probable that the waste will be available for free. Basalt in Poland occurs mainly in Lower Silesia and a small part in the Opole voivodeship [23]. Their location in both voivodeships is shown below in Figure 1 [24]. Figure 1 reproduced permission from Ref. [25]. Basalts used for this research come from two different open-pit mines located in Lower Silesia. This area is located across several geological formations: the Pre-Sudetic Block, the southwestern fragment of the Pre-Sudetic Monocline and the Sudetic Block, excluding a part of the Eastern Sudetes. They were formed as a result of Cenozoic block movements [26]. Basalt extracted from these mines is used to produce asphalt. Larger fractions are used as asphalt ballast, while small fractions are utilized as one of the components of the mix used for bituminous pavement. It is added to asphalt mixture due to its high toughness [27]. Since the products tested here were covered by trade secrets, they were named basalt dust A and basalt dust B. Chemical composition of basalt received from an open-pit mine A is shown in Table 1. Table 2 contain results of granulometric analysis implemented for basalt dust A. Basalt dust B's chemical composition is given in Tables 3 and 4 contains granulometric analysis for basalt dust B. An example of rock from which basalt dust was obtained is shown in Figure 2. Figure 3 shows the basalt B dust used in the study. Authors did not find much information about the impact of basalt dust on thermal conductivity of cement slurries. These were probably some of the first studies on the effect of basalt dust on the thermal conductivity of grouts. Furthermore, not much information was found about the strength properties of grouts after adding basalt dust.

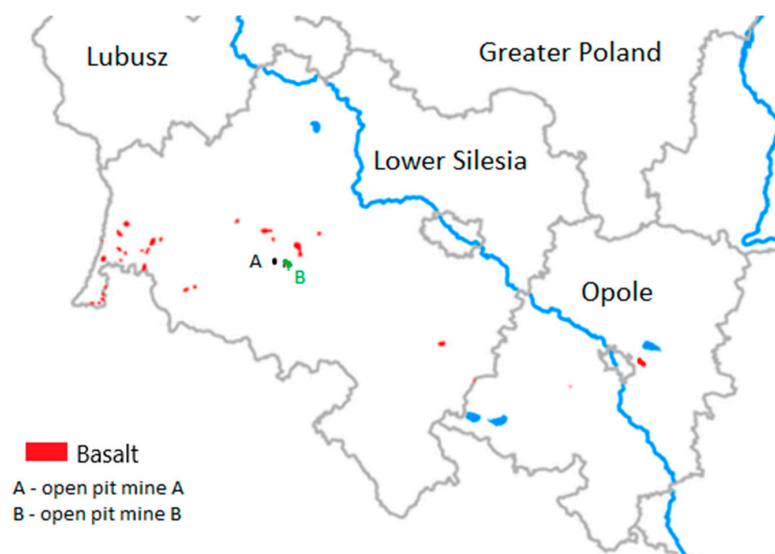


Figure 1. Location of basalt deposits from which basalt dust is obtained in Poland [23].



Figure 2. Basalt rock from open-pit mine (photo by K. Seńczuk).



**Figure 3.** Basalt dust (photo by K. Seńczuk).

**Table 1.** Basalt A chemical composition.

Composition	Content %
[-]	[%]
Roasting loss	$2.08 \pm 0.08$
SiO <sub>2</sub>	$42.38 \pm 0.46$
Al <sub>2</sub> O <sub>3</sub>	$11.29 \pm 0.19$
Fe <sub>2</sub> O <sub>3</sub>	$12.69 \pm 0.19$
CaO	$1.22 \pm 0.19$
MgO	$13.19 \pm 0.19$
SO <sub>3</sub>	$0.07 \pm 0.05$
Na <sub>2</sub> O	$2.47 \pm 0.13$
K <sub>2</sub> O	$1.17 \pm 0.09$
P <sub>2</sub> O <sub>5</sub>	$0.61 \pm 0.06$
TiO <sub>2</sub>	$2.50 \pm 0.11$
Mn <sub>2</sub> O <sub>3</sub>	$0.24 \pm 0.05$
SrO	$0.08 \pm 0.06$
ZnO	$0.02 \pm 0.05$

**Table 2.** Results of granulometric analysis for basalt dust A.

Mesh Size	Weight	% by Mass
[mm]	[g]	[%]
0.300	42.005	8.160
0.180	82.605	16.050
0.150	85.190	16.550
0.125	80.950	15.730
0.106	71.910	13.970
0.075	62.600	12.160
0.063	33.495	6.510
0.056	15.400	2.990
0.050	10.906	2.120
0.040	8.536	1.660
0.032	19.565	3.800
0.025	1.053	0.200
0.020	0.552	0.110
<0.200	0.003	0.001

The results shown in Table 2 were obtained for two samples of about 515 g each. Samples spent 24 h in the oven before testing.

**Table 3.** Basalt B chemical composition.

Composition	Content
[-]	[%]
Roasting loss	1.02 ± 0.08
SiO <sub>2</sub>	46.37 ± 0.55
Al <sub>2</sub> O <sub>3</sub>	14.53 ± 0.19
Fe <sub>2</sub> O <sub>3</sub>	11.86 ± 0.11
CaO	9.49 ± 0.09
MgO	8.21 ± 0.05
SO <sub>3</sub>	0.00 ± 0.05
Na <sub>2</sub> O	3.70 ± 0.13
K <sub>2</sub> O	1.33 ± 0.17
P <sub>2</sub> O <sub>5</sub>	0.62 ± 0.05
TiO <sub>2</sub>	2.54 ± 0.05

**Table 4.** Results of granulometric analysis for basalt dust.

Mesh Size	Weight	% by Mass
[mm]	[g]	[%]
0.300	36.200	7.030
0.180	80.840	15.700
0.150	95.760	18.600
0.125	83.950	16.310
0.106	69.910	13.580
0.075	60.525	11.760
0.063	34.495	6.700
0.056	14.400	2.810
0.050	6.360	1.240
0.040	7.130	1.390
0.032	23.565	4.580
0.025	1.215	0.240
0.020	0.375	0.070
<0.200	0.005	0.001

Furthermore, laboratory study has been conducted to check the effect of basalt dust A on the strength of hardened grouts after 28 days in water. By hardened slurry, the authors mean slurry that has changed from a liquid state to a solid state after being poured into a mold. Samples were tested in view of compressive and flexural strength. Laboratory testing of cement slurry strength is important because insufficient grout strength can lead to hole destruction. Strength testing has been described in the literature for both oil and geothermal wells. Strength increasing and strength decreasing additives have been studied [28–49]. So far, strength-enhancing additives include materials such as:

- Eggshell powder (ESP) [28];
- Quartz sand [29];
- Loose silica dust [30];
- Microsilica [31];
- Graphene [32];
- Ground granulated blast furnace slag (GGBS) [33,34];
- Nanosilica fume (NSF) [35];
- Silica fume (SF) [36];
- Nanosilica [37];
- Diatomite [38];
- Hblock [39];
- NanoSiO<sub>2</sub> [40];
- Slag [41];
- Nano-Al<sub>2</sub>O<sub>3</sub> (NA) [42];

- Halloysite [43];
- N, N, N', N'-tetramethyl ethylenediamine (TEMED) (99%) [44];
- Mix of polypropylene (PP) fiber and glass (G) fiber [45];
- Cellulose nanocrystals (CNC), cellulose nanofibrils (CNF), bacterial cellulose (BC) and cellulose filaments (CF) [46,47];
- Marble slurry powder (MSP) [48];
- Tailings (such as granite cutting waste) [49].

## 2. Materials and Methods

The thermal conductivity coefficient is a very sensitive parameter. During testing, the final result can be affected by, e.g., a temporary change in outdoor temperature or a change in room humidity. The amount of thermal conductivity is also affected by, e.g., the structure or density of the material [50].

The entire process from the execution of the laboratory test to obtained analysis results can be divided into three parts:

- The first part involved making the grout mixtures and pouring the disc-shaped molds and rectangular molds. All disk-shaped samples were placed in containers with water for 28 days. In case of beams being included in basalt dust B, parts of the samples were tested immediately after hardening. The others were placed in containers filled with water for 28 days. Cement slurries consisted of water, cement and an additive (basalt dust A and basalt dust B). Preparation of cement grout is trivial. As an example, to prepare 5 samples with a water–mix ratio of between 0.5 and 10% basalt dust content, 300 g of water, 540 g of cement and 60 g of dust are required. Firstly, water was added to a clean container and placed under the stirrer, and then cement and dust were weighed and mixed. When stirring started, it was important that no air bubbles formed and the cement/dust mixture was added slowly. Well mixed slurry was poured into disc-shaped moulds. Mold shape depended on the kind of laboratory tests, such as strength and thermal conductivity analysis. Thermal conductivity testing required circle/disc shape samples while strength tests required beams with dimensions of 40 × 40 × 160 mm.
- The second stage began after 28 days and involved performing thermal conductivity tests using a FOX 50 instrument.
- The last part was based on the segregation and analysis of all the results obtained.

All tested grout mixtures were based on Portland cement with the trade name Cement premium 42,5R found in the catalog of Góraźdże Cement S.A.

Approximately 280 disc-shaped samples and about 320 beams were prepared and tested.

### 2.1. Materials

Two materials were needed for the study: Portland cement and basalt dust. They are described below.

CEM I 42,5 R was commonly used Portland cement compliant with PN-EN 197-1:2012 standard. It is easily available on the market, which encourages a low price [51].

Basalt dust was obtained by crushing basalt blocks in crushers. The rocks from which the dust was obtained were characterized by high strength, high melting point, acid resistance, resistance to low temperatures and were a low-flammability material [52]. The main difference between dusts A and B was that in dust A, sunburn does not occur. Sunburn is an unusual type of basaltoid disintegration that develops immediately throughout the rock. This occurs usually as bright, mostly gray or russet spots. Basalt dust B was obtained from basalt deposits located nearby Winnica hill. Winnica hill is located in Piotrowice, a village located in the Lower Silesia voivodeship. The basaltoids located on the hill belong to the young alpine basalt formations of the platform foreground of the European Alps. They extend from Saxony and the Rhine through Bohemia, Lower Silesia, Opole and Moravia. In Germany, the Czech Republic and Poland, they form isolated clusters called spot concentrations [53]. In the region of the Czech massif and the Sudetes, the

concentrations are spaced about 80–85 km apart, have similar diameters of 35–45 km and form the Czech-Silesian volcanic arc. The age of these basaltoids is determined to be Lower to Middle Oligocene. Basalt dust A was obtained from an open-pit mine located near Złotoryja in the Lower Silesia voivodeship. There was a small difference in the composition of dusts A and B. The biggest difference in chemical composition was the content of  $\text{SiO}_2$ ,  $\text{Al}_2\text{O}_3$ ,  $\text{CaO}$ ,  $\text{MgO}$ ,  $\text{Na}_2\text{O}$  and roasting loss. Dust A had more  $\text{SiO}_2$  (about 4%),  $\text{Al}_2\text{O}_3$  (3.24%) and  $\text{Na}_2\text{O}$  (1.23%), whereas dust B contained more  $\text{CaO}$  (1.72%) and  $\text{MgO}$  (about 5%). Only differences greater than 1% were considered in this comparison.

## 2.2. Description of Thermal Conductivity Tests

About 280 thermal conductivity tests were performed on disc-shaped samples. The FOX 50 device was used for this purpose. The device consisted of two plates positioned in parallel, between which sealant samples were placed in the form of discs. These plates protected the sample during testing. This apparatus allows conductivity tests to be performed in the temperature range between 10 and 110 °C. The FOX 50 requires a cooling device and a compressor for proper operation. The cooling device helps maintain constant temperatures during testing. Figure 4 shows the FOX 50 apparatus and instruments used for tests. Figure 5 presents one of the disc-shape samples used for thermal conductivity testing [53]. All samples spent 24 h indoors under constant conditions before testing. All 5 samples of the same concentration were always tested on the same day.

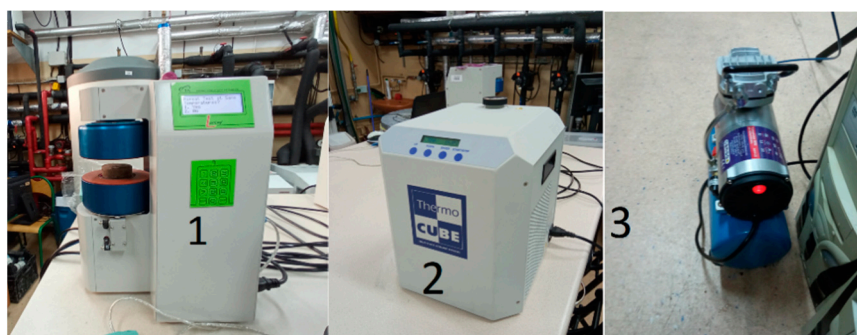


**Figure 4.** FOX 50 aperture with instrumentation. (1) LambdaMeter FOX 50; (2) ThermoCube 200–500 Solid State Cooling System cooler; (3) compressor DED7472 Derda (photo by K. Seńczuk).



**Figure 5.** Disc-shaped samples were used to check thermal conductivity (photo by K. Seńczuk).

The device is quite complicated when it comes to determining the final result of the conductivity value for samples. One block of data appearing on the device consists of 256 cycles that last approximately 4 min 20 s. The results of each block include the temperature on the lower and upper plates, and the signals from the lower transducers. These values are compared with the average values of the previous blocks. If this comparison meets all of the following criteria, the thermal equilibrium of the sample is considered to have been reached, ending the test for that block. All criteria are shown below.

- (a) Temperature equilibrium criterion (T.E. criterion);
- (b) Semi-equilibrium criterion (S.E. criterion);
- (c) Percentage equilibrium criterion (P.E. criterion);
- (d) Inflexion criterion.

Only when all 4 criteria are met can results be calculated. The final result is obtained as the average value of the last three blocks. Precision of the FOX 50 device is about 3%. The results are shown to 4 decimal places, which is the same order of accuracy relative to the accuracy of the calibration standard materials [54].

To calculate thermal conductivity coefficient  $\lambda$  [ $\frac{W}{m \cdot K}$ ], FOX 50 uses the following Equation (1) [54]:

$$\lambda = \frac{\Delta x}{\left[ \frac{\Delta T}{(S_{cal} \cdot Q) - 2 \cdot R} \right]} \quad (1)$$

where  $\Delta x$ —sample thickness [m];  $\Delta T$ —temperature gradient between upper and lower plate [K];  $S_{cal}$ —proportionality factor between transducer output signal and heat flux [ $W \cdot m^{-2} \mu V^{-1}$ ];  $Q$ —output signal in transducer [ $\mu V$ ];  $R$ —thermal contact resistance [ $m^2 \cdot K \cdot W^{-1}$ ].

### 2.3. Description of Strength Tests

Basalt dusts A and B were used as an additive to cement slurry for all assumed water–mix ratios and their effect on the strength of the hardened Portland cement after 28 days in water was tested. Basalt dust B was also tested for its effect on strength immediately after setting. For each dust concentration, five  $40 \times 40 \times 160$  mm beams were made. Figure 6 shows the device used in strength tests. Examples of beams used in strength tests are located in Figures 7 and 8.



Figure 6. Matest model E—183PN100 (photo by K. Seńczuk).



Figure 7. Beam used in flexural strength test (photo by K. Seńczuk).



Figure 8. Samples used in compressive strength tests (photo by K. Seńczuk).

The Matest apparatus model E—183PN100 by Matest company located in Treviolo BG, Italy consisted of two chambers and a control device. The beam was placed in the left chamber, then the flexural strength option was selected on the control device. If necessary, the sample dimensions in the settings were changed, and then the instrument was started.



Beams were placed in the right chamber, then the compressive strength option was selected on the control and the test began. After starting, the device increased the force that put pressure on the sample. Testing ended when the beam broke (this refers to flexural and compressive strength tests). The results were obtained to three decimal places. According to the manufacturer’s instructions, the device does not use any equations to determine strength values.

### 3. Results

In this section of the article, data obtained from the laboratory research are presented and analyzed. Ten different grouts concentrations were prepared for both thermal conductivity coefficient ( $\lambda$ ) and strength tests. The additive contents used in tested cement-basal dust mixes were 0%; 1%; 2.5%; 5%; 7.5%; 10%; 20%; 30%; 40% and 50% BWOC (by weight of cement). For thermal response tests and both strengths, five samples were made for each concentration of basalt dust. For concentrations in which significant differences in either strength or thermal conductivity values occurred, additional tests were performed. The updated data obtained after additional tests were introduced. Additional tests were performed for concentrations where there was too much variation in results. The “results” section includes updated data.

#### 3.1. Thermal Conductivity Test

Tables 5–7 and Figures 9–11 summarize the average values of the thermal conductivity coefficient and contain the results obtained for basalt dust A for water–mix ratios 0.5, 0.6 and 0.7, respectively. Similarly, results for basalt dust B are included in Tables 8–10 and Figures 12–14 for water–mix ratios 0.5, 0.6 and 0.7. The thermal conductivity coefficient values in Figures 9–11 are presented to 3 decimal places. For the purpose of testing the thermal conductivity coefficient, about 280 disks were made and tested.

**Table 5.** Average thermal conductivity for basalt dust A for all samples for water –mix ratio = 0.5.

Thermal Conductivity $\lambda$ [ $\frac{W}{mk}$ ]	
Minimum	0.571
Maximum	0.721
Median	0.600
Average	0.606
Standard deviation	0.042
The range of variation	0.146

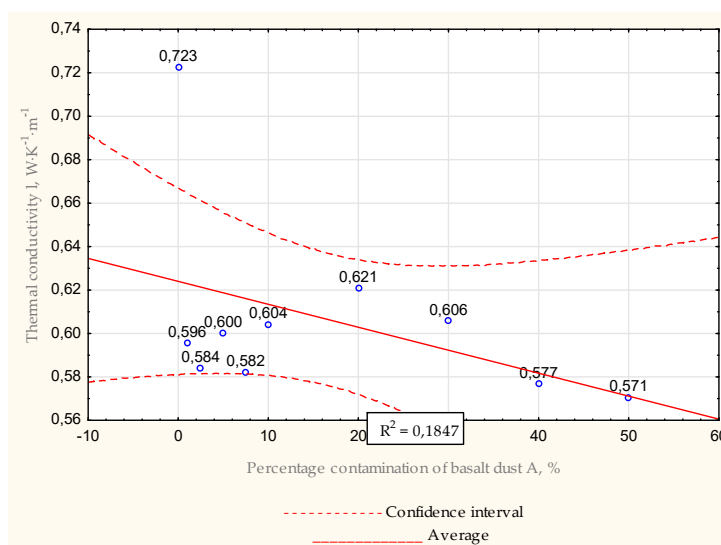


**Figure 9.** Average thermal conductivity for basalt dust A for water –mix ratio = 0.5.

As can be seen in Figure 9, all samples containing basalt dust A as an additive had lower thermal conductivity values than the zero sample. The lowest value was obtained for the slurry with 50% dust content. In this case, the thermal conductivity value was about 21% lower than that of the zero sample. For remaining grout mixtures, values were lower by about 14% to 20%.

**Table 6.** Average thermal conductivity for basalt dust A for all samples for water –mix ratio = 0.6.

Thermal Conductivity $\lambda$ [ $\frac{W}{mk}$ ]	
	Statistics
Minimum	0.497
Maximum	0.721
Median	0.616
Average	0.618
Standard deviation	0.063
The range of variation	0.225

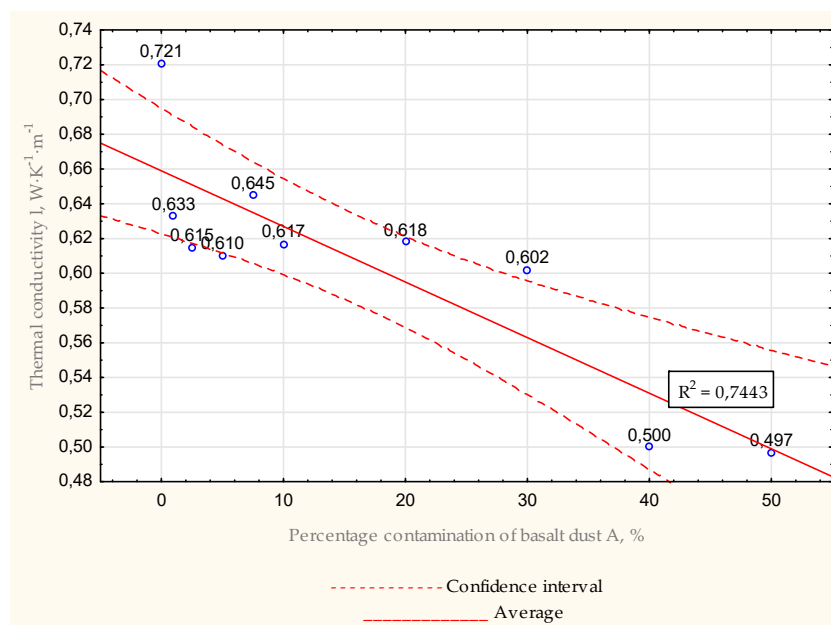


**Figure 10.** Average thermal conductivity for basalt dust A for water –mix ratio = 0.6.

Figure 10 indicates that, similar to Figure 9, the thermal conductivity values of the samples containing basalt dust were lower than those of the zero sample. Here, the lowest conductivity value occurred for the formula containing 50% dust in the mixture. For this sample, the thermal conductivity coefficient was about 31% lower than the zero sample value. For the rest of the grout mixtures, decreases in thermal conductivity values varied between 10% and 30%.

**Table 7.** Average thermal conductivity for basalt dust A for all samples for water –mix ratio = 0.7.

Thermal Conductivity $\lambda$ [ $\frac{W}{mk}$ ]	
	Statistics
Minimum	0.505
Maximum	0.634
Median	0.586
Average	0.573
Standard deviation	0.039
The range of variation	0.129

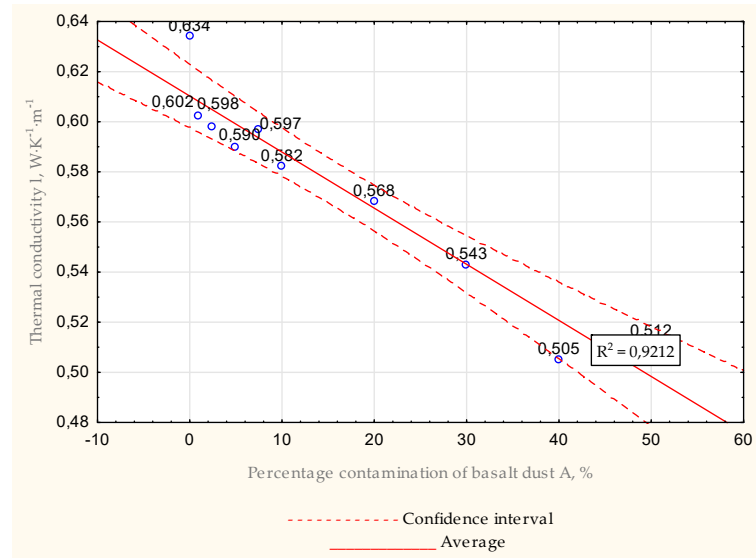


**Figure 11.** Average thermal conductivity for basalt dust A for water –mix ratio = 0.7.

Analysis of the results for basalt dust A with a water mix–ratio = 0.7 shows a decreasing trend in the value of the thermal conductivity. This trend occurred as the concentration of basalt dust in the slurry increased. The lowest value of thermal conductivity was obtained for the sample containing 40% basalt dust in its composition. The value of the thermal conductivity coefficient in this case was lower than that of the zero sample by almost 20%. For the remaining samples, reduction varied by about 5% to 19%.

**Table 8.** Average thermal conductivity for basalt dust B for all samples for water –mix ratio = 0.5.

	Thermal Conductivity λ [ $\frac{W}{mk}$ ]
Minimum	0.482
Maximum	0.628
Median	0.588
Average	0.586
Standard deviation	0.040
The range of variation	0.146

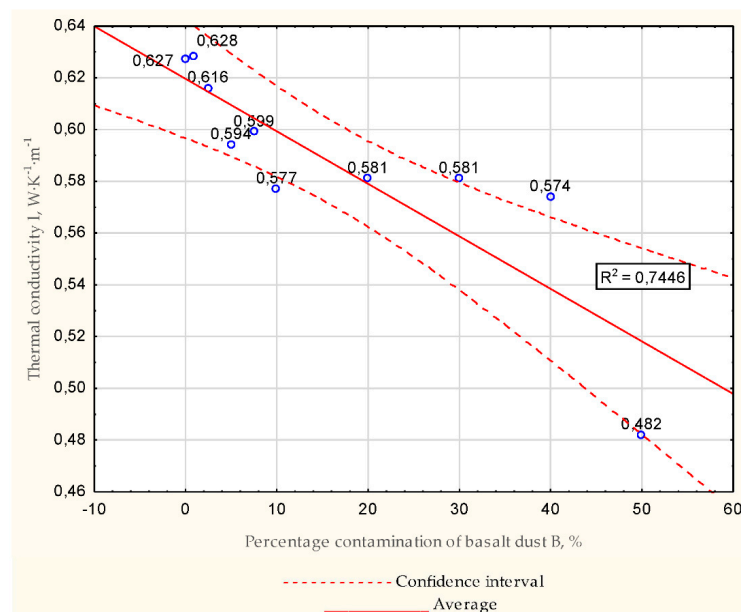


**Figure 12.** Average thermal conductivity for basalt dust B for water –mix ratio = 0.5.

According to Figure 12, the slurries with dust content of 1% had values about 0.1% greater than the zero sample. For remaining concentrations, a decrease in thermal conductivity values was observed. The decreases in these values varied from about −1.7% to about −23% compared to the zero sample. The lowest conductivity value was found for the grout with a basalt dust content of 50%.

**Table 9.** Average thermal conductivity for basalt dust B for all samples for water –mix ratio = 0.6.

Thermal Conductivity $\lambda$ [ $\frac{W}{mk}$ ]	
	Statistics
Minimum	0.566
Maximum	0.677
Median	0.623
Average	0.625
Standard deviation	0.034
The range of variation	0.111

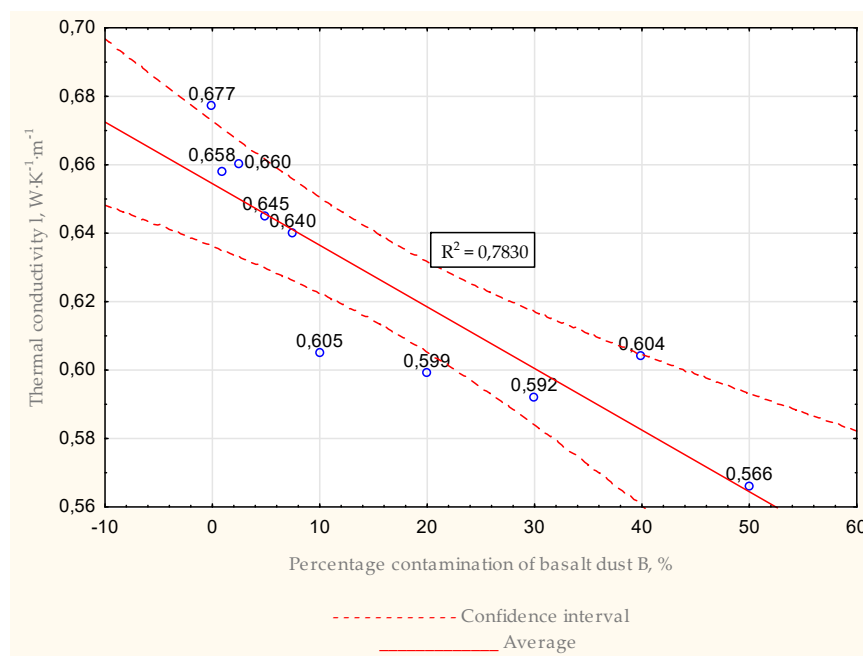


**Figure 13.** Average thermal conductivity for basalt dust B for water –mix ratio = 0.6.

Data contained in Table 9 again shows a decreasing trend in the value of the thermal conductivity coefficient. All samples containing basalt B dust as an additive had thermal conductivity values less than those of the zero sample. The lowest value was observed for the grout with a dust content of 50%; in this case the thermal conductivity value was about 16% lower than that of the zero sample. For other grout mixtures, the thermal conductivity coefficient was about 3% to 12.5% lower.

**Table 10.** Average thermal conductivity for basalt dust B for all samples for water –mix ratio = 0.7.

Thermal Conductivity $\lambda$ [ $\frac{W}{mk}$ ]	
	Statistics
Minimum	0.581
Maximum	0.659
Median	0.614
Average	0.615
Standard deviation	0.022
The range of variation	0.078

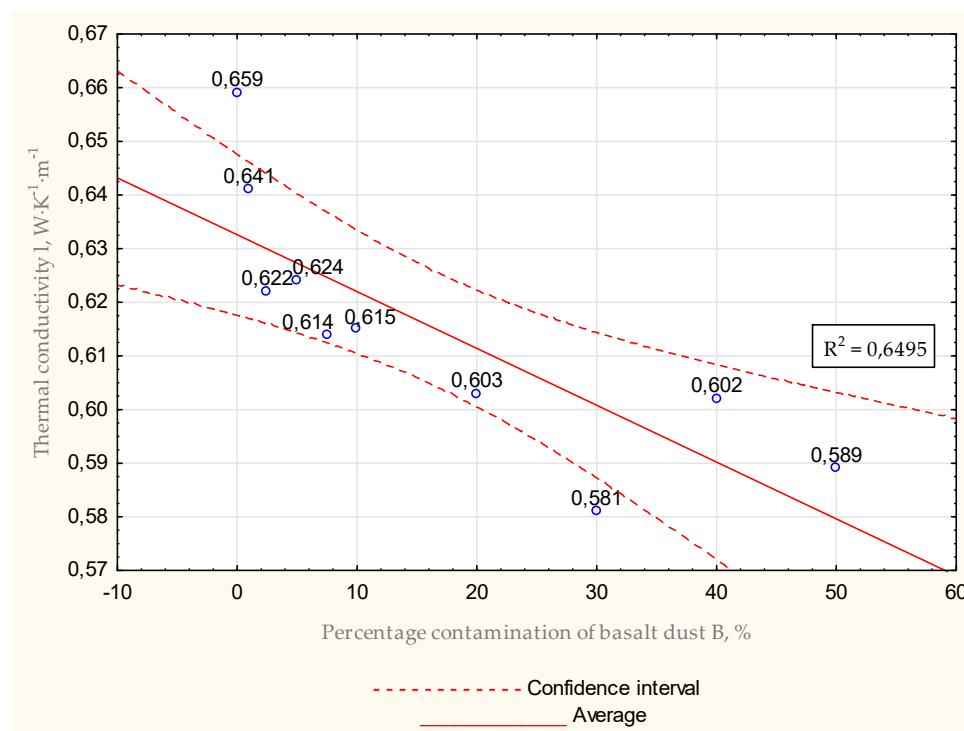


**Figure 14.** Average thermal conductivity for basalt dust B for water –mix ratio = 0.7.

Upon analysis of the data in Table 10, the trend of decreasing thermal conductivity values relative to the zero sample was again noted. Once again for basalt dust B, all grout mixtures had lower values of thermal conductivity compared to the base specimen. The lowest thermal conductivity value was found for samples containing this additive at 30%. In this case, the thermal conductivity value compared to the zero sample was about 12% lower. For all remaining grout mixtures, the thermal conductivity coefficient was about 2.5% to 10% lower.

Thermal conductivity coefficient tests require a very strict, repeatable (under the same conditions) experimental procedure since many factors influence the final test results. Cement slurry must be prepared carefully. Care should be taken when mixing dry ingredients with water to avoid the formation of vortices that would allow air to enter the freshly prepared grout.

### 3.2. Flexural and Compressive Strength Tests

The effect of basalt dust on the strength of depletion grouts was tested. These tests are very important because for geothermal wells as well as deep borehole heat exchangers, the strength of cement slurry is a parameter equally important as thermal conductivity. If the grout strength is too low, the function of the borehole may be adversely affected, and the borehole may fail [6,55]. For this reason, strength values at least equal to the zero sample are required. Two types of strength tests were performed on the hardened samples: flexural strength, and compressive strength. In both cases, the maximum force and maximum pressure are given. For each water–cement ratio of 0.5, 0.6 and 0.7, respectively, the results are collected in two tables. Tables 11–16 contains both strengths results. Tables 11, 13 and 15 show flexural strength test results. Tables 12, 14 and 16 include compressive strength tests. Figures 15, 16, 19, 20, 23 and 24 show the results obtained from the flexural strength tests and Figures 17, 18, 21, 22, 25 and 26 show the results from the compressive strength tests. Tables 11–16 and Figures 15–26 refer to the results obtained for basalt dust A. For the purpose of strength testing, about 320 beams were made and tested.

**Table 11.** Flexural strength tests for basalt dust A for all samples for water –mix ratio = 0.5.

	Maximum Strength [kN]	Maximum Press Force [MPa]
	Statistic	
Minimum	2.333	5.641
Maximum	4.634	10.465
Median	4.063	9.441
Average	3.787	8.745
Standard deviation	0.753	1.632
The range of variation	2.301	4.824

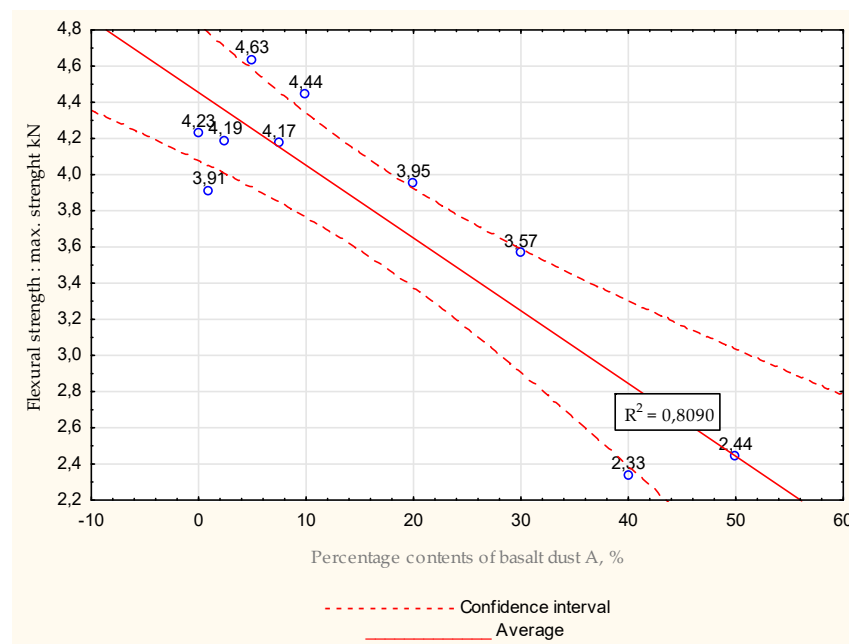


**Figure 15.** Average values received during flexural strength tests for water –mix ratio = 0.5, maximal strength.

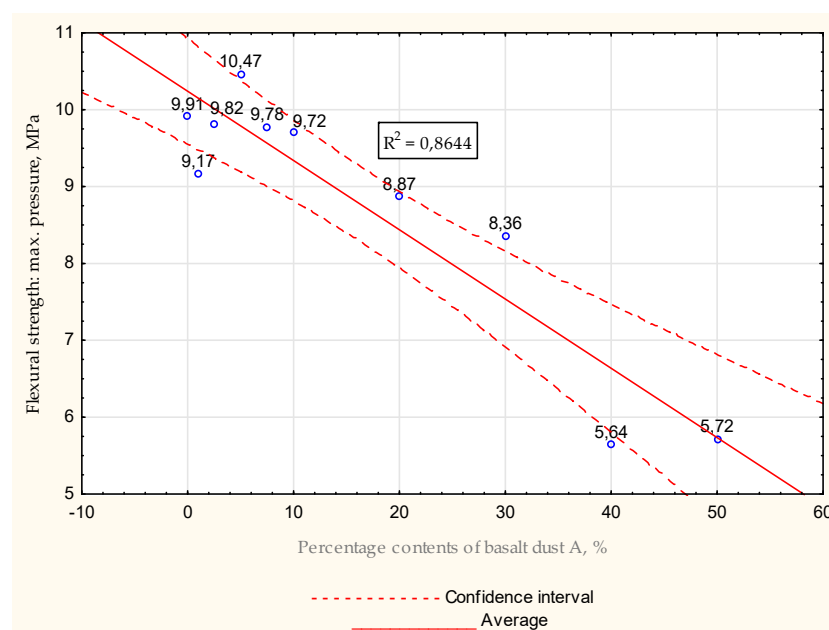


**Figure 16.** Average values received during flexural strength tests for water –mix ratio = 0.5, maximal pressure.

Figures 15 and 16 show that there was a decreasing trend in strength values as the concentration of additive in the grout increased. Hardened slurries containing dust with a concentration of 40% had flexural strength values reduced by approximately 43%. For other samples, the reduction in strength values varied between 16% for a concentration of 1% and 18% for a dust content of 30%.

**Table 12.** Compressive strength tests for basalt dust A for all samples for water –mix ratio = 0.5.

	Maximum Strength [kN]	Maximum Press Force [MPa]
Statistic		
Minimum	30.526	18.599
Maximum	78.696	47.127
Median	71.259	44.240
Average	64.061	39.238
Standard deviation	17.027	10.257
The range of variation	48.170	28.528

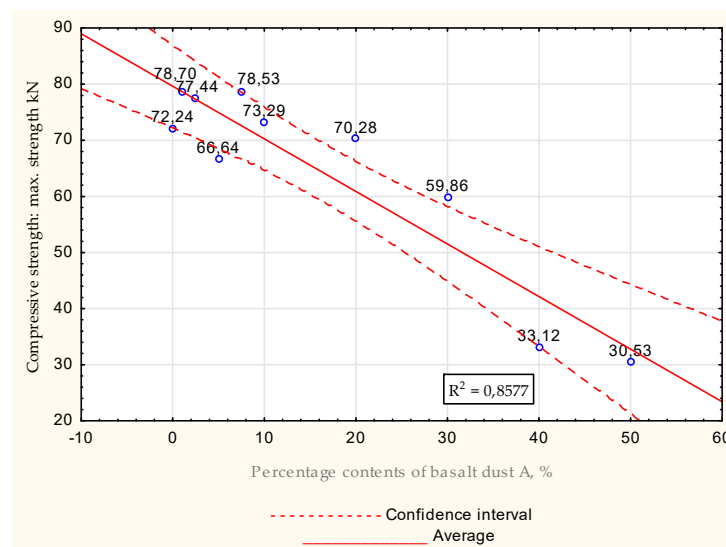


**Figure 17.** Average values received during compressive strength tests for water –mix ratio = 0.5, max. strength.

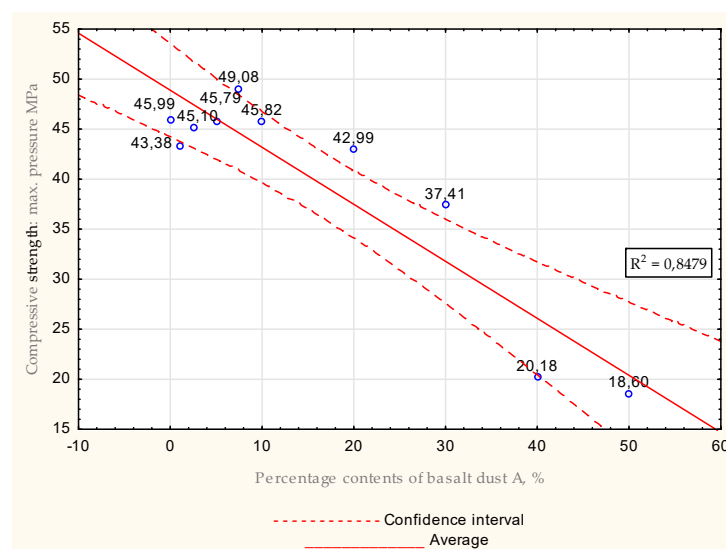


**Figure 18.** Average values received during compressive strength tests for water –mix ratio = 0.5, max. pressure.

Compressive strength values again showed a decreasing trend in strength with increasing basalt dust concentration. The lowest strength value was obtained for the sample containing 40% basalt dust, for which the strength value was 55% lower than that of the zero sample. In the remaining samples, the reduction in conductivity values varied by a maximum of 11%.

For a water –mix ratio of 0.5, there was a decreasing trend in flexural and compressive strength values for formulations containing dust concentrations of 10% and above for both strength tests.

**Table 13.** Flexural strength tests for basalt dust A for all samples for water –mix ratio = 0.6.

	Maximum Strength [kN]	Maximum Press Force [MPa]
	Statistic	
Minimum	1.286	3.340
Maximum	4.145	9.715
Median	3.309	7.756
Average	3.186	7.450
Standard deviation	0.913	2.025
The range of variation	2.860	6.375

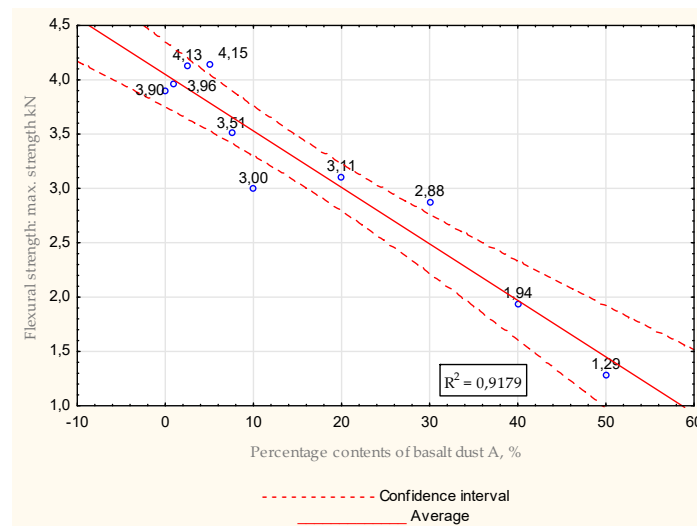


**Figure 19.** Average values received during flexural strength tests for water –mix ratio = 0.6, maximal strength.

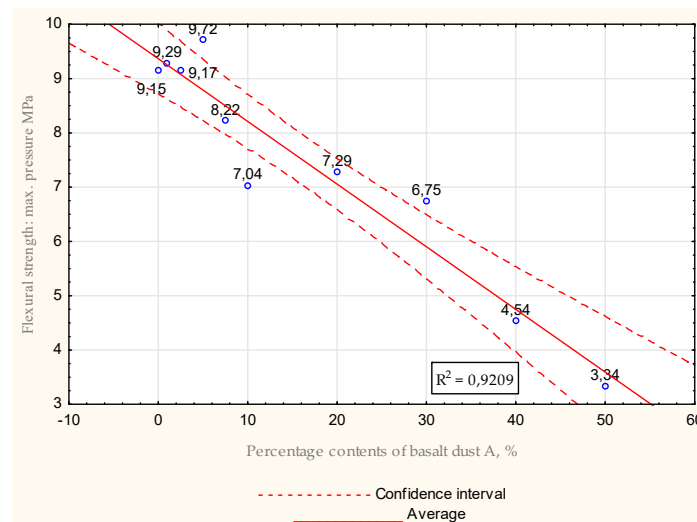


**Figure 20.** Average values received during flexural strength tests for water –mix ratio = 0.6.



For water –mix ratio 0.6, for samples with an additive concentration above 7.5%, there was a trend of decreasing flexural and compressive strength values as the additive concentration of the grout increased. For flexural strength, it was noted that increased strengths occurred for formulations with low additive contents of 1%, 2.5% and 5%. Comparing the values of these strengths to those of the zero sample, it can be seen that the difference was a maximum of 15%. For samples that had dust concentrations of 7.5% and above in their composition, the values of flexural strength decreased by up to 26%.

**Table 14.** Compressive strength tests for basalt dust A for all samples for water –mix ratio = 0.6.

	Maximum Strength [kN]	Maximum Press Force [MPa]
Statistic		
Minimum	16.116	10.073
Maximum	59.736	37.243
Median	45.249	28.850
Average	42.185	26.758
Standard deviation	12.401	7.747
The range of variation	43.620	27.170

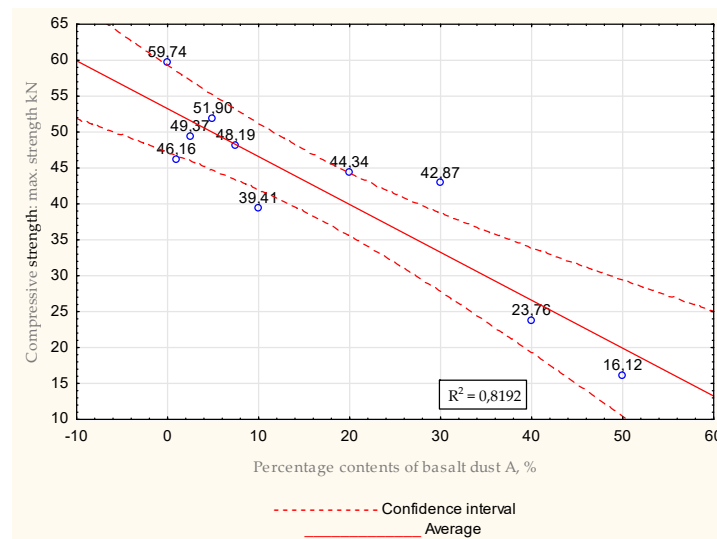


**Figure 21.** Average values received during compressive strength tests for water –mix ratio = 0.6, maximal strength.

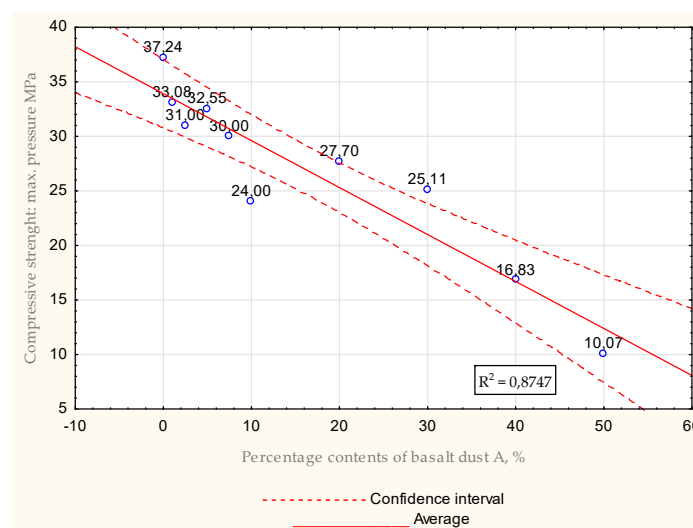


**Figure 22.** Average values received during compressive strength tests for water –mix ratio = 0.6, maximal pressure.

The compressive strength values of the cement slurries for all tested formulas were lower than those of the zero sample. The closest to the zero sample was the formula containing 5% dust in its composition, for which the values were about 1.5% lower. For the other samples, the compressive strength values were reduced in the range of 6–37% compared to the zero sample.

**Table 15.** Flexural strength tests for basalt dust A for all samples for water –mix ratio = 0.7.

	Maximum Strength [kN]	Maximum Press Force [MPa]
	Statistic	
Minimum	1.660	3.890
Maximum	2.701	5.713
Median	2.364	5.336
Average	3.314	5.226
Standard deviation	0.264	0.494
The range of variation	1.041	1.823

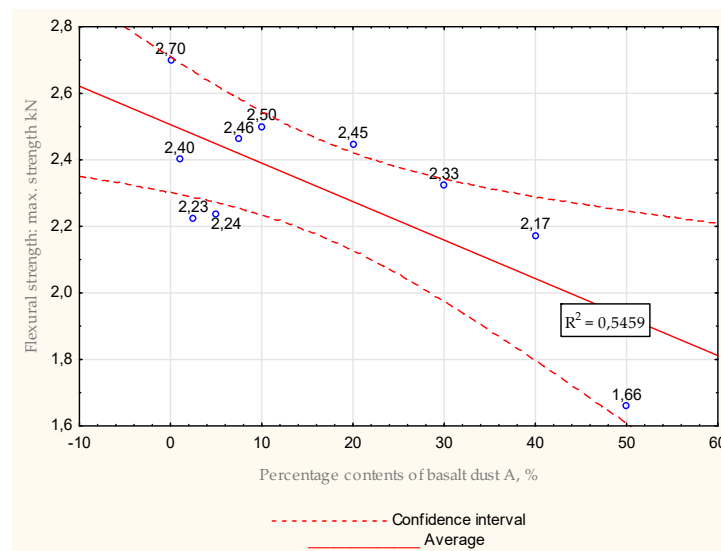


**Figure 23.** Average values obtained during flexural strength tests for water –mix ratio = 0.7, maximal strength.

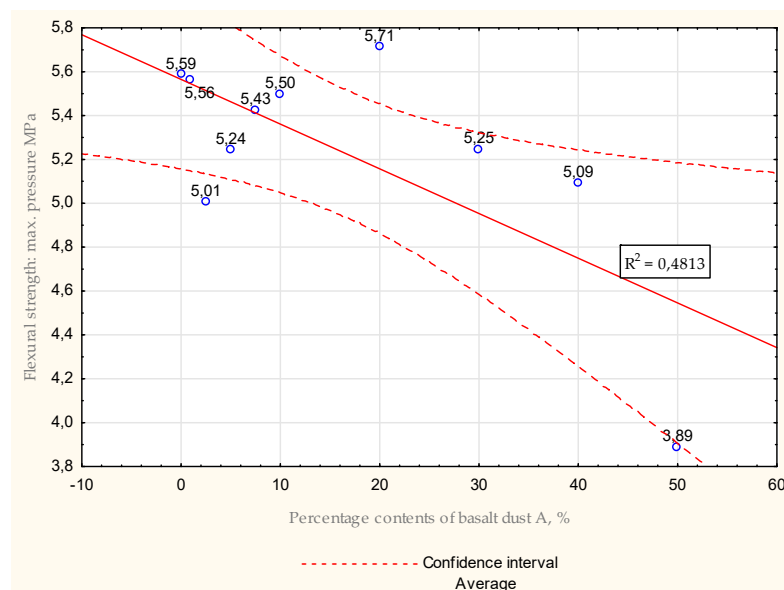


**Figure 24.** Average values obtained during flexural strength tests for water –mix ratio = 0.7, maximal pressure.

For a water –mix ratio of 0.7, an overall decreasing trend was observed. The greatest reduction in flexural strength values was observed for samples with an additive concentration of more than 20% basalt dust A in the sealing grout. Samples with dust concentrations of 1%, 7.5%, 10% and 20% had increased flexural strength values compared to the zero sample. However, the difference in these values was small and did not exceed 12%. Such an increase may be due to uneven mixing of the additive in the sample.

**Table 16.** Compressive strength tests for basalt dust A for all samples for water –mix ratio = 0.7.

	Maximum Strength [kN]	Maximum Press Force [MPa]
	Statistic	
Minimum	18.444	11.528
Maximum	30.074	24.483
Median	27.884	19.086
Average	27.004	19.043
Standard deviation	3.312	3.578
The range of variation	11.630	12.955

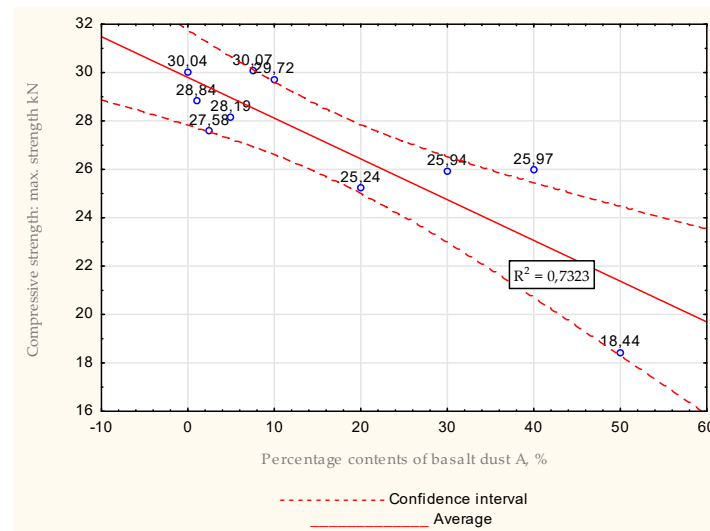


**Figure 25.** Average values obtained during compressive strength tests for water –mix ratio = 0.7, maximal strength.

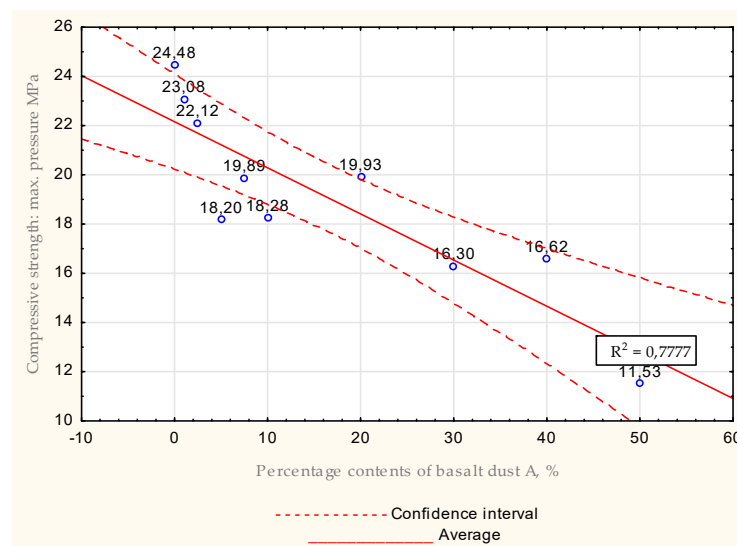


**Figure 26.** Average values obtained during compressive strength tests for water –mix ratio = 0.7.

The compressive strength values of basalt A dust cement slurries also showed a decreasing trend with increasing additive value. The lowest compressive strength value was obtained for a dust concentration of 30%. Comparing it to the zero sample value, it was about 41% lower. For the other concentrations, the reduced compressive strength values were lower compared to the zero sample value by up to 40%.

Samples having similar or higher strength values than the zero sample can be successfully used as a replacement for cement components.

All tables (Tables 17–22) and figures (Figures 27–38) presented below concern basalt dust B.

Tables 17, 19 and 21 and Figures 27, 28, 31, 32, 35 and 36 present data obtained during flexural strength tests. Tables 18, 20 and 22 and Figures 29, 30, 33, 34, 37 and 38 include compressive strength tests results. Tables 17–22 and Figures 27–38 describe samples which lay 28 days in containers filled with water.

**Table 17.** Flexural strength tests for basalt dust B for all samples for water –mix ratio = 0.5 after 28 days.

	Maximum Strength [kN]	Maximum Press Force [MPa]
	Statistic	
Minimum	2.363	5.538
Maximum	4.173	9.782
Median	3.430	7.724
Average	3.330	7.668
Standard deviation	0.539	1.241
The range of variation	1.810	4.244

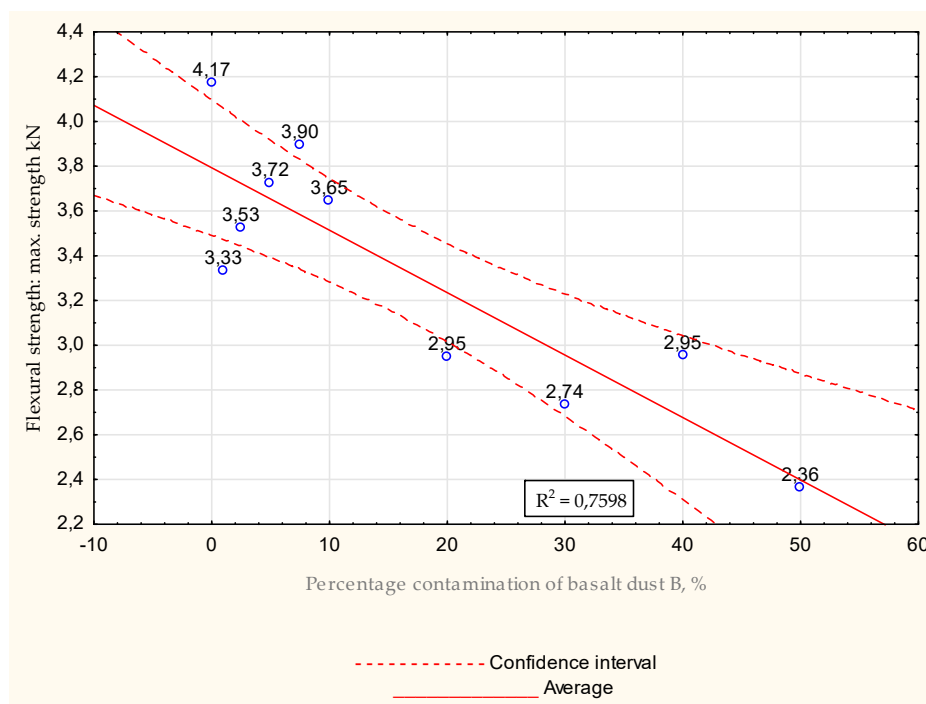


**Figure 27.** Average values obtained during flexural strength tests after 28 days for water –mix ratio = 0.5, maximal strength.

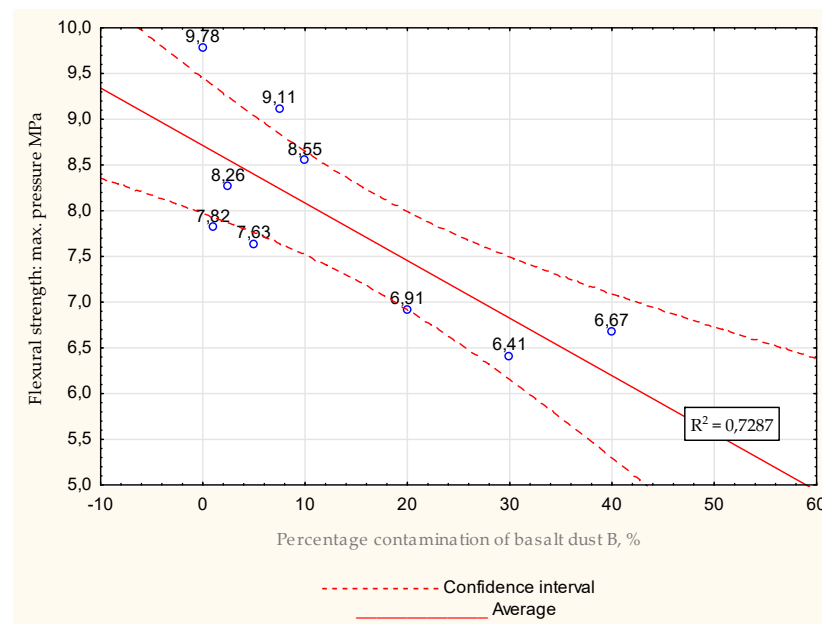


**Figure 28.** Average values obtained during flexural strength tests after 28 days for water –mix ratio = 0.5, maximal pressure.

For water–mix ratio 0.5, once again a decreasing trend was observed.

For flexural strength tests, the lowest value was obtained for samples with 50% basalt dust. The value was about 43% lower than that of the zero sample. Remaining grout mixtures had lower results, which varied between 6% and about 34%.

**Table 18.** Compressive strength tests for basalt dust B for all samples for water –mix ratio = 0.5 after 28 days.

	Maximum Strength [kN]	Maximum Press Force [MPa]
	Statistic	
Minimum	26.969	16.855
Maximum	69.891	42.930
Median	58.413	36.508
Average	52.838	33.038
Standard deviation	13.498	8.265
The range of variation	42.922	28.075

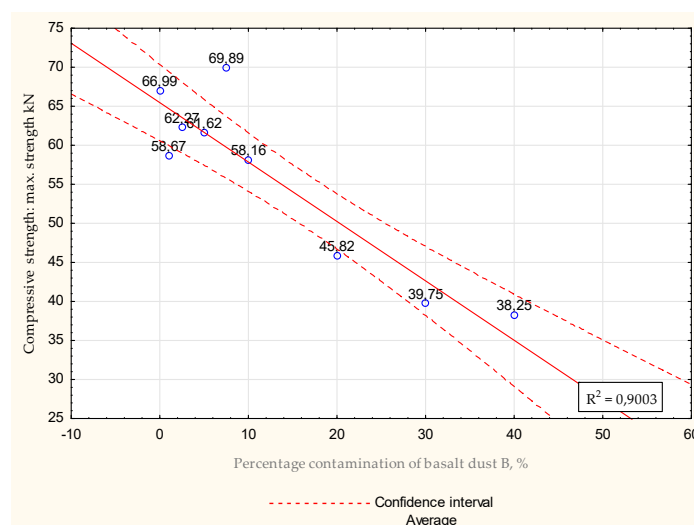


**Figure 29.** Average values obtained during compressive strength tests after 28 days for water –mix ratio = 0.5, max. strength.

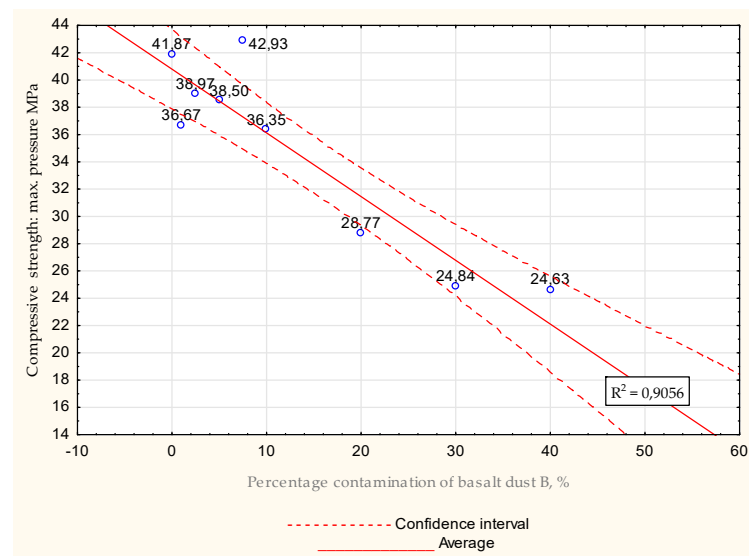


**Figure 30.** Average values obtained during compressive strength tests after 28 days for water –mix ratio = 0,5, max. pressure.

Almost all results obtained from compressive strength tests were lower than those of the zero sample. The lowest value was obtained for contamination of basalt dust of 50%, which decreased its strength by about 60%. For remaining results the difference varied between 7% and 42%.

**Table 19.** Flexural strength tests for basalt dust B for all samples for water –mix ratio = 0.6 after 28 days.

	Maximum Strength [kN]	Maximum Press Force [MPa]
	Statistic	
Minimum	1.315	3.089
Maximum	3.093	7.248
Median	2.801	6.564
Average	2.561	5.987
Standard deviation	0.604	1.414
The range of variation	1.778	4.159

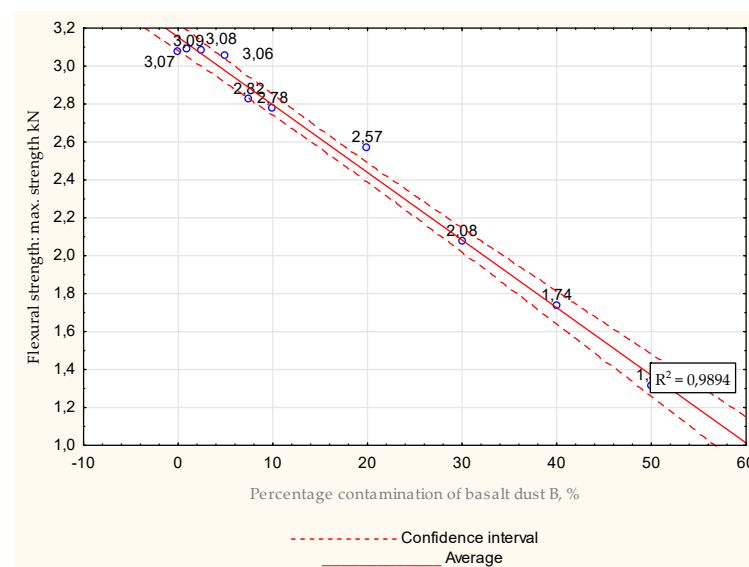


**Figure 31.** Average values obtained during flexural strength tests after 28 days for water –mix ratio = 0,6, maximal strength.

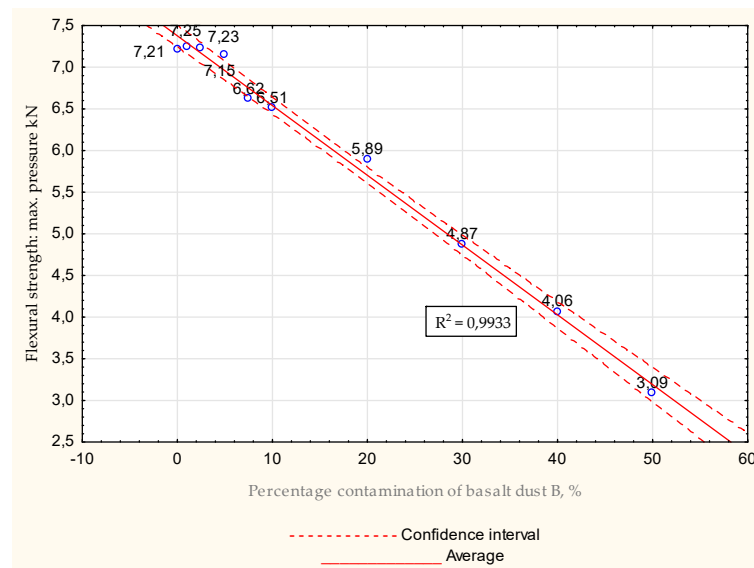


**Figure 32.** Average values obtained during flexural strength tests after 28 days for water –mix ratio = 0.6, maximal pressure.

As can we see above, the data obtained from flexural strength tests for the water–mix ratio 0.6 present a decreasing trend in strength values as basalt dust concentration in slurry increased. The lowest value was obtained for grout mixture with 50% additive in its composition. For it, the result was about 57% lower. In other cases, differences varied by about +0.33% to about –43.5%.

**Table 20.** Compressive strength tests for basalt dust B for all samples for water –mix ratio = 0.6 after 28 days.

	Maximum Strength [kN]	Maximum Press Force [MPa]
	Statistic	
Minimum	13.957	8.346
Maximum	52.373	32.733
Median	44.001	27.467
Average	37.354	22.808
Standard deviation	12.838	8.014
The range of variation	38.416	24.387

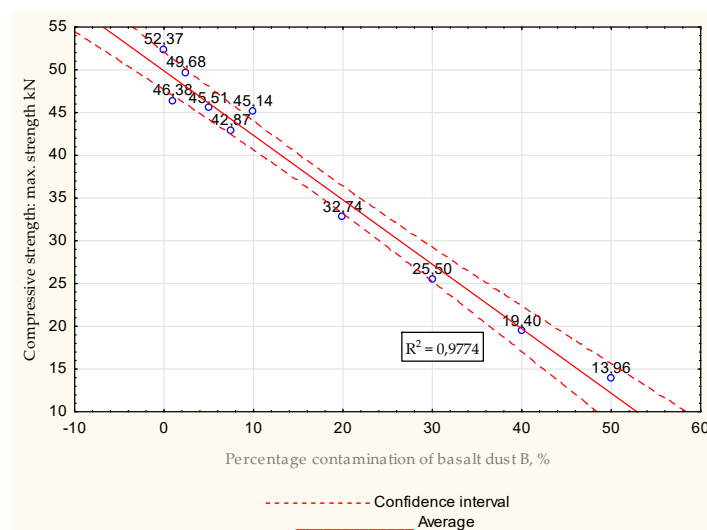


**Figure 33.** Average values obtained during compressive strength tests after 28 days for water –mix ratio = 0.6, max. strength.

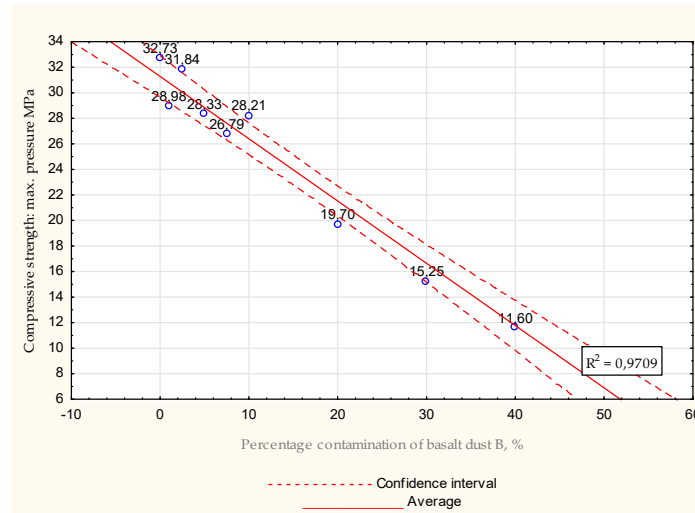


**Figure 34.** Average values obtained during compressive strength tests after 28 days for water –mix ratio = 0.6, max. pressure.

For compressive strength tests, all grout mixtures had lower values than the zero sample. The lowest result was obtained for an additive concentration of 50%, whose value was about 74% lower. For remaining samples, the reduction varied between 5% and 63%.

**Table 21.** Flexural strength tests for basalt dust B for all samples for water –mix ratio = 0.7 after 28 days.

	Maximum Strength [kN]	Maximum Press Force [MPa]
	Statistic	
Minimum	1.272	2.962
Maximum	2.495	5.685
Median	2.057	4.926
Average	1.978	4.818
Standard deviation	0.374	0.695
The range of variation	1.223	2.723

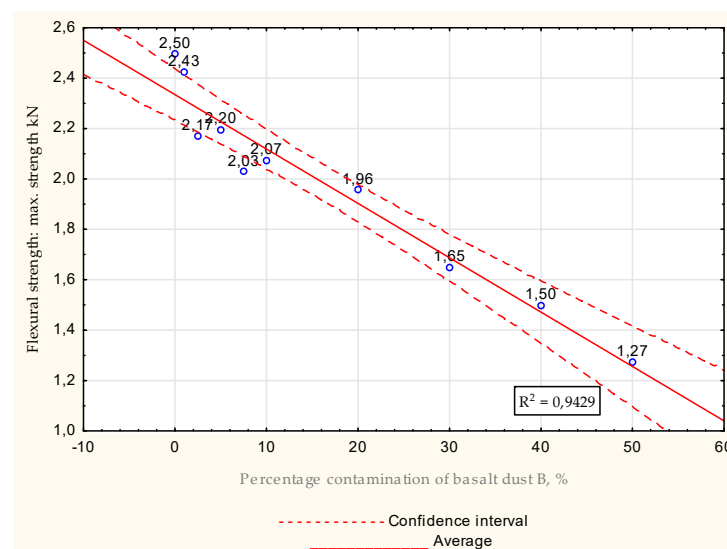


**Figure 35.** Average values obtained during flexural strength tests after 28 days for water –mix ratio = 0.7, maximal strength.



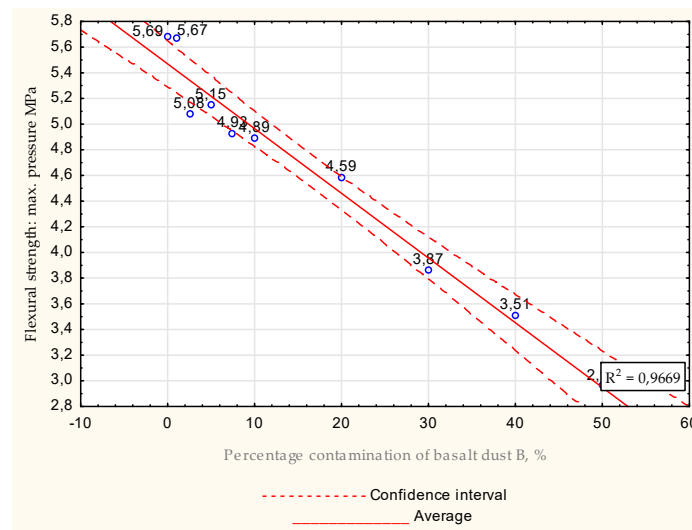


**Figure 36.** Average values obtained during flexural strength tests after 28 days for water –mix ratio = 0.7, maximal pressure.

For water–mix ratio 0.7, flexural strength values once again showed a trend of decreasing strength. For both max. strength and max. pressure, the lowest value was obtained for the mixture with 50% basalt dust. Results were about 49% lower for max. strength and about 48% lower for max. pressure compared to those of the base slurry. For the remaining samples, the reduction in values varied between 0.2% and 40%.

**Table 22.** Compressive strength tests for basalt dust B for all samples for water –mix ratio = 0.7 after 28 days.

	Maximum Strength [kN]	Maximum Press Force [MPa]
	Statistic	
Minimum	12.770	7.981
Maximum	30.586	18.292
Median	25.108	15.016
Average	23.079	13.880
Standard deviation	5.421	3.122
The range of variation	17.816	10.311

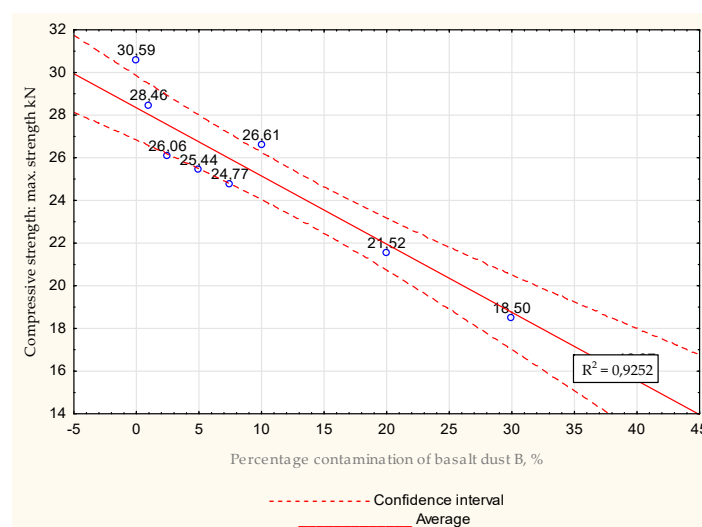


**Figure 37.** Average values obtained during compressive strength tests after 28 days for water –mix ratio = 0.7, max. strength.

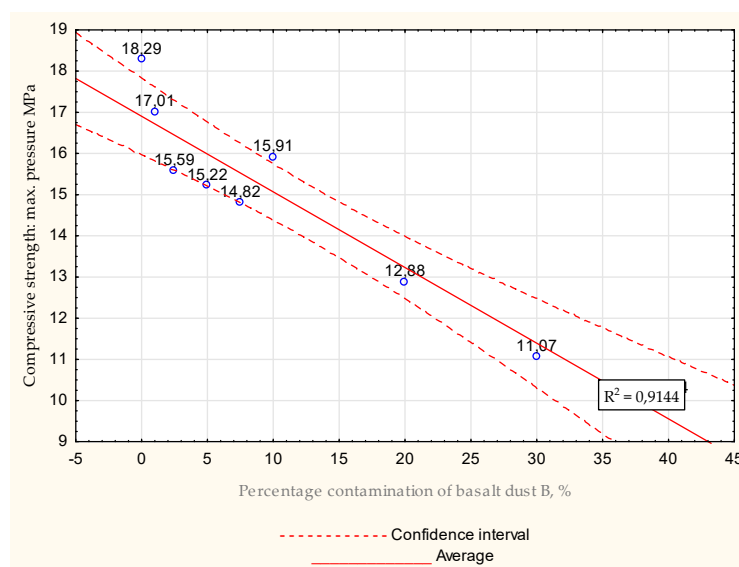


**Figure 38.** Average values obtained during compressive strength tests after 28 days for water –mix ratio = 0.7, max. pressure.

Similar to those for flexural strength, compressive strength test results showed decreasing values with an increased concentration of basalt dust. The lowest value was obtained for samples with 50% additive. The decrease in strength was about 58% compared to the zero sample. For other grout mixtures, the decrease in values varied between  $-7\%$  and  $-47\%$ .

#### 4. Discussion

Two different basalt dusts were tested. Tests were performed to examine thermal conductivity, flexural strength and compressive strength. Approximately 280 disc-shaped samples (thermal conductivity) and about 320 beams (compressive strength and flexural strength) were prepared and tested. Tests were performed for three different water–mix ratio values, 0.5, 0.6 and 0.7, for a wide range of dust percentage concentrations that ranged from 1% to 50% relative to BWOC (by weight of cement).

Analysis of the results obtained from the thermal conductivity tests for dust A showed a trend of decreasing value with increasing additive concentration in the slurry. All comparisons of the results obtained relate to individual concentrations in relation to the zero sample. The water mix 0.5 results presented in Figure 9 show that the lowest thermal conductivity was obtained for mixtures consisting of 50% basalt dust. For others, results were about 14–20% lower. Water–mix ratios 0.6 (Figure 10) and 0.7 (Figure 11) showed similar trends to those of water–mix 0.5. As expected, for basalt dust B all water–mix ratios showed trends of reduced thermal conductivity values with increasing additive concentration in the slurry. The largest differences in values were for water–mix ratio 0.5 for the grout with a dust content of 50%. This value was about 23% lower compared to the zero sample. The differences in thermal conductivity values may result from the fact that the thermal conductivity test is very sensitive. The results obtained were influenced by such factors as, e.g., temperature, humidity, air circulation and material structure. Compressive strength and compression tests were also performed. For each tested sample two results were obtained: max. pressure and max. force. For both basalt dusts, we can see decreasing values of compressive and flexural strength with increasing additive concentration in the slurry. Analysis of the obtained data showed that with an increase in the water–mix ratio, the strength values decreased. This correlation occurs for both basalt dusts. For flexural strength, the biggest decrease between concentrations occurred for water–mix 0.5 (basalt dust A) which can be noted in Figure 16. For basalt dust B, not all samples were within the assumed confidence intervals. In Figure 23 samples with dust concentrations 2.5%, 5%

and 20% were off assumed intervals. This means that they should not be considered as additives for use in the geothermal industry.

For basalt dust A, the lowest values were obtained for samples containing 50% additives. Of all three water–mix coefficients, the samples for water–mix 0.6 had the lowest value. Larger decreases in values occurred from concentrations of 40%. This applies to both flexural and compressive strengths.

For basal dust B, for all three water–mixture ratios there was a notable decrease in strength values for samples containing basalt dust in amounts of 20% or more. This correlation occurred for both compressive and flexural strengths for all samples which spent 28 days in water. The lowest values were obtained for the samples containing minimum 40% basal dust B.

For compressive strength, in both dusts a certain correlation can be observed. For water–mix ratio 0.5, the value for a concentration of 50% was about 60% lower, for 0.6 about 70%, and for 0.7 about 40%, respectively. Analysis of the flexural strength results revealed a similar correlation for both basalt dusts. For water–mix ratio 0.5, the lowest value was about 40% less, for 0.6 about 65% and for 0.7 about 35%, respectively.

As can be seen in the case of basalt A dust, significant drops in values occurred at concentrations of 40% and 50%. In contrast, for basalt dust B, these decreases occurred at concentrations of 20% and more. This may be due to the fact that, as mentioned earlier, basalt dust A was obtained from rocks that were not sunburnt.

Cement grouts with values lower than  $0.5 \text{ W}\cdot\text{K}^{-1}\cdot\text{m}^{-1}$  can be successfully used in the cementing process for DBHE near the surface to reduce the heat released from holes. Low thermal conductivity grouts also can be used for cementing geothermal wells along the entire length to minimize heat losses. Most preferable are grouts with increased strength values. Too low a strength can lead to damage or complete destruction of the borehole. Grouts that had strength reduced by up to 10% relative to the zero sample are suitable to use.

## 5. Conclusions

- There is a growing interest in technologies that use heat from different depths below the ground or geothermal water. It may be crucial to look for ways of reducing the cost of making such installations. One possibility is to use commonly available and inexpensive materials when preparing grout. This material could be used as a substitute for cement or as an additive to increase or decrease thermal conductivity values;
- The effect of two different basalt dusts on the conductivity and strength of the formulas were tested. The deciding factors were no information about similar studies previously conducted, environmental safety and the fact that these dusts are considered waste. Tested basalt dusts were obtained as a waste product from the mining of basalt aggregate and can be used in cement grouts;
- Approximately 280 disc-shaped samples and about 320 beams were prepared and tested. Tests were performed for three different water–mix ratio values, 0.5, 0.6 and 0.7, for a wide range of dust percentage concentrations that ranged from 1% to 50% relative to BWOC (by weight of cement). For some beams, variations of the results obtained were too high. Therefore, these samples were again made and tested;
- Analysis of the obtained results indicates a decrease in the value of the heat conductivity coefficient with an increased percentage concentration of dust. This trend was shown for basalt dust A and dust B. In comparison to the value of the zero sample, the thermal conductivity of the compositions containing a concentration of 50% of dust A decreased by no more than 31.07%, and for dust B by a max. 23.13%;
- Thermal conductivity is a parameter which is very sensitive and is susceptible to changes in surroundings. The factor that influenced the thermal conductivity results is the accuracy of mixing the additive in the slurry and the distribution of the additive particles in the hardened sample. For this reason, proper, reproducible preparation of the cementitious slurry is very important. Attention must be paid to the conditions

under which dry ingredients are mixed with water and to the correct procedure when pouring fresh grout into molds. Thermal conductivity is also strongly dependent on environmental conditions, i.e., temperature and humidity. During testing, the moisture content of the samples was maximized due to curing conditions—an environment similar to that of the borehole was assumed, i.e., full immersion in water;

- Grouts with the addition of basalt dust, which lowers the value of thermal conductivity, may find application mainly in cementing of geothermal wells at their full depth and in cementing of deep borehole heat exchangers in the near-surface sections of boreholes. The addition of dust as a cement replacement ingredient should also be considered. The cost of cements should be lower;
- All samples with strength values higher or equal to the zero sample can be successfully used for geothermal wells and at the surface layers of deep borehole heat exchangers;
- Analysis of the obtained results indicates a decrease of both flexural and compressive strength. This trend was shown for basalt dust A and dust B in comparison to the value of the zero sample. However, one should be cautious when considering the use of cementitious grouts with concentrations above 20%, both as a cement replacement and as an additive to reduce conductivity. The boundary values for their use depend on grout strengths.

**Author Contributions:** Conceptualization, K.S. and T.K.; methodology, K.S. and A.S.-Ś.; software, K.S.; validation, K.S.; formal analysis, K.S.; investigation, K.S.; resources, K.S. and T.K.; data curation, K.S.; writing—original draft preparation, K.S.; writing—review and editing, A.S.-Ś.; visualization, K.S.; supervision, A.S.-Ś.; project administration, A.S.-Ś.; funding acquisition, A.S.-Ś. All authors have read and agreed to the published version of the manuscript.

**Funding:** This research was funded by The National Centre for Research and Development, Program Applied research implemented under the Norwegian Financial Mechanism 2014–2021/POLNOR2019, grant number NOR/POLNOR/BHEsINNO/0018/2019-00, AGH UST agreement no. 28.28.190.70190 (50%) and Program “Excellence Initiative-Research University” for the AGH University of Science and Technology (50%).

**Institutional Review Board Statement:** Not applicable.

**Informed Consent Statement:** Not applicable.

**Data Availability Statement:** Not applicable.

**Conflicts of Interest:** The authors declare no conflict of interest.

## References

1. Sheng, P.; Yanlong, K.; Chen, C.; Pang, Z.; Wang, J. Optimization of the utilization of deep borehole heat exchangers. *Geotherm. Energy* **2020**, *8*, 6. [[CrossRef](#)]
2. Sapińska-Śliwa, A.; Rosen, M.A.; Gonet, A.; Śliwa, T. Deep Borehole Heat Exchangers—A Conceptual Review. In Proceedings of the World Geothermal Congress 2015, Melbourne, Australia, 19–25 April 2015.
3. Alberti, L.; Angelotti, A.; Antelmi, M.; La Licata, I. A numerical study on the impact of grouting material on borehole heat exchangers performance in aquifers. *Energies* **2017**, *10*, 703. [[CrossRef](#)]
4. Blazquez, C.S.; Martín, A.F.; Nieto, I.M.; García, P.C.; Sanchez Perez, L.S.S.; Gonzalez-Aguilera, D. Analysis and study of different grouting materials in vertical geothermal closed-loop systems. *Renew. Energy* **2017**, *114*, 1189–1200. [[CrossRef](#)]
5. Chicco, J.M.; Mandrone, G. How a sensitive analysis on the coupling geology and borehole heat exchanger characteristics can improve the efficiency and production of shallow geothermal plants. *Heliyon* **2022**, *8*, e09545. [[CrossRef](#)]
6. Dubiel, S.; Śliwa, T.; Kowalski, T.; Stryczek, S.; Wiśniowski, D.; Bieda, A.; Piwowarczyk, S.; Beszlej, J.; Naklicki, M. The impact of diatomite on the thermal conductivity of solidified grout. *AGH Drill. Oil Gas* **2017**, *34*, 3. [[CrossRef](#)]
7. Śliwa, T.; Ciepiewska, M. Cement Slurries with Modified Thermal Conductivity for Geothermal Applications. In Proceedings of the 47th Workshop on Geothermal Reservoir Engineering, Stanford University, Stanford, CA, USA, 7–9 February 2022.
8. Sapińska-Śliwa, A. Effectiveness of heat Recovery from Rock Mass in the Context of the Production Method by Means of Boreholes. *Dissertation monographs 364*, Doctor of Science thesis, AGH Publishers, Krakow, Poland, 2019.
9. Delaleux, F.; Py, X.; Olives, R.; Dominguez, A. Enhancement of geothermal borehole heat exchangers performances by improvement of bentonite grouts conductivity. *Appl. Therm. Eng.* **2012**, *33–34*, 92–99. [[CrossRef](#)]

10. Berktaş, I.; Nejad Ghafar, A.; Fontana, P.; Caputcu, A.; Menciloglu, Y.; Saner Okan, B. Synergistic Effect of Expanded Graphite-Silane Functionalized Silica as a Hybrid Additive in Improving the Thermal Conductivity of Cementitious Grouts with Controllable Water Uptake. *Energies* **2020**, *13*, 3561. [CrossRef]
11. Berktaş, I.; Nejad Ghafar, A.; Fontana, P.; Caputcu, A.; Menciloglu, Y.; Saner Okan, B. Facile Synthesis of Graphene from Waste Tire/Silica Hybrid Additives and Optimization Study for the Fabrication of Thermally Enhanced Cement Grouts. *Molecules* **2020**, *25*, 886. [CrossRef]
12. Chen, Y.-J.; Nguyen, D.-D.; Shen, M.-Y.; Yip, M.-C.; Nyan-Hwa Tai, N.-H. Thermal characterizations of the graphite nanosheets reinforced paraffin phase-change composites. *Compos. Part A Appl. Sci. Manuf.* **2013**, *44*, 40–46. [CrossRef]
13. Śliwa, T.; Sowa, M.; Stryczek, S.; Gonet, A.; Złotkowski, A.; Sapińska-Śliwa, A.; Knez, D. Badania stwardniałych zaczynów cementowych z dodatkiem grafitu (The study of hardened cement slurries with addition of graphite). *Wiert. Naft. Gaz* **2011**, *28*, 571–585 (In Polish). (In Polish)
14. Li, B.; Zhang, J.; Yan, H.; Liu, H.; Zhu, C. Thermal enhancement of gangue-cemented paste backfill with graphite and silica sand: An experimental investigation. *Environ. Sci. Pollut. Res.* **2022**, *29*, 49050–49058. [CrossRef]
15. Wang, S.; Jian, L.; Shu, Z.; Chen, S.; Chen, L. A High Thermal Conductivity Cement for Geothermal Exploitation Application. *Nat. Resour. Res.* **2022**, *29*, 6. [CrossRef]
16. Śliwa, T.; Kowalski, T.; Cekus, D.; Sapińska-Śliwa, A. Research on Fresh and Hardened Sealing Slurries with the Addition of Magnesium Regarding Thermal Conductivity for Energy Piles and Borehole Heat Exchangers. *Energies* **2021**, *14*, 5119. [CrossRef]
17. Zhang, N.; She, W.; Du, F.; Xu, K. Experimental Study on Mechanical and Functional Properties of Reduced Graphene Oxide/Cement Composites. *Materials* **2020**, *13*, 3015. [CrossRef]
18. Zhu, Y.; Qin, Y.; Liang, S.; Chen, K.; Tian, C.; Wang, J.; Luo, X.; Zhang, L. Graphene/SiO<sub>2</sub>/n-octadecane nanoencapsulated phase change material with flower like morphology, high thermal conductivity, and suppressed supercooling. *Appl. Energy* **2019**, *250*, 98–108. [CrossRef]
19. Wang, S.; Li, Y.; Wu, L.; He, X.; Jian, L.; Chen, Q. Investigation on thermal conductivity property and hydration mechanism of graphene-composite cement for geothermal exploitation. *Geothermics* **2022**, *104*, 102477. [CrossRef]
20. Cho, J.; Waetzig, G.R.; Udayakantha, M.; Hong, C.Y.; Banerjee, S. Incorporation of Hydroxyethylcellulose- Functionalized Halloysite as a Means of Decreasing the Thermal Conductivity of Oilwell Cement. *Sci. Rep.* **2018**, *8*, 16149. [CrossRef]
21. Sikora, P.; Abd Elrahman, M.; Horszczaruk, E.; Brzozowski, P.; Stephan, D. Incorporation of magnetite powder as a cement additive for improving thermal resistance and gamma-ray shielding properties of cement-based composites. *Constr. Build. Mater.* **2019**, *204*, 113–121. [CrossRef]
22. Lou, T.; Pei, P.; Chen, Y.; Hao, D.; Wang, C. Improvements in the Water Retention Characteristics and Thermophysical Parameters of Backfill Material in Ground Source Heat Pumps by a Molecular Sieve. *Energies* **2022**, *15*, 1801. [CrossRef]
23. Kozieł, M. The characteristics of national basalts of dolnośląski region with the purpose of amorphous fiber. *Prace Instytutu Szkła, Ceramiki, Materiałów Ogniotrwałych i Budowlanych 2009/R.*; 4/4, 55–64. YADDA ID: bwmeta1.element.baztech-article-BTB2-0070-0088. Available online: <http://yadda.icm.edu.pl/baztech/element/bwmeta1.element.baztech-article-BTB2-0070-0088> (accessed on 14 July 2022).
24. Szwed-Lorenz, M. Basalt—A stone for various purposes. In Proceedings of the XV Seminar Methodology of Prospecting and Documenting Mineral Deposits and Geological Services for Mines, Augustów, Poland, 28–30 May 2014.
25. Majtyka, T. Available online: [https://pl.wikipedia.org/wiki/Plik:PL\\_bazalt\\_z%C5%82o%C5%BCa.png](https://pl.wikipedia.org/wiki/Plik:PL_bazalt_z%C5%82o%C5%BCa.png) (accessed on 22 February 2022).
26. Don, J.; Żelaźniewicz, A. The Sudetes—Boundaries, subdivisions and tectonic patterns. *Neues Jahrbuch Geol. Paläont. Abh.* **1990**, *179*, 121–127.
27. Radzidzewski, P.; Sarnowski, M.; Plewa, A.; Pokorski, P. Properties of asphalt concrete with basalt-polymer fibers. *Arch. Civ. Eng.* **2018**, *64*, 4. [CrossRef]
28. Murtaza, G.; Tunio, A.H.; Bhatti, M.A.; Sargani, E.H. Designing of Cement Slurry to Enhance Compressive Strength and Rheology: An Experimental Study. *Int. J. Curr. Eng. Technol.* **2021**, *11*, 2. [CrossRef]
29. Liu, L.; Cai, G.; Liu, X.; Liu, S.; Puppala, A.J. Evaluation of thermal-mechanical properties of quartz sand-bentonite-carbon fiber mixtures as the borehole backfilling material in ground source heat pump. *Energy Build.* **2019**, *202*, 109407. [CrossRef]
30. Kremieniewski, M. Grout mixture of Lightweight Slurry with High Early Strength of the Resultant Cement Sheath. *Energies* **2020**, *13*, 1583. [CrossRef]
31. Renjun, X.; Zhiqiang, W.; Xiaowei, C.; Xiucheng, N. Research on the Mechanical Integrity of Low-Density Cement Mortar. *Front. Mater.* **2022**, *8*, 837348. [CrossRef]
32. Śliwa, T.; Sapińska-Śliwa, A.; Wysogład, T.; Kowalski, T.; Konopka, I. Strength Tests of Hardened Cement Slurries for Energy Piles, with the Addition of Graphite and Graphene, in Terms of Increasing the Heat Transfer Efficiency. *Energies* **2021**, *14*, 1190. [CrossRef]
33. Munjal, P.; Kong, K.H.; Cheng Chuen Hon, A. Effect of GGBS and curing conditions on strength and microstructure properties of oil well cement slurry. *J. Build. Eng.* **2021**, *40*, 102331. [CrossRef]
34. Reddy Suda, V.B.; Srinivasa Rao, P. Experimental investigation on optimum usage of Micro silica and GGBS for the strength characteristics of concrete. *Mater. Today* **2020**, *27*, 805–811. [CrossRef]
35. Li, B.; Zhang, J.; Yan, H.; Zhou, N.; Li, M. Experimental investigation into the thermal conductivity of gangue-cemented paste backfill in mine application. *J. Mater. Res. Technol.* **2022**, *16*, 1792–1802. [CrossRef]

36. Zheng, S.; Liu, T.; Qu, B.; Fang, C.; Li, L.; Feng, Y.; Jiang, G.; Yu, Y. Experimental investigation on the effect of nano silica fume on physical properties and microstructural characteristics of lightweight cement slurry. *Constr. Build. Mater.* **2022**, *329*, 127172. [[CrossRef](#)]
37. Banar, R.; Dashti, P.; Zolfagharnasab, A.; Ramezaniapour, A.M.; Ramezaniapour, A.A. A comprehensive comparison between using silica fume in the forms of water slurry or blended cement in mortar/concrete. *J. Build. Eng.* **2022**, *46*, 103802. [[CrossRef](#)]
38. Bayanak, M.; Zarinabadi, S.; Shahbazi, K.; Azimi, A. Effects of Nano Silica on oil well cement slurry characteristics and control of gas channeling. *S. Afr. J. Chem. Eng.* **2020**, *34*, 11–25. [[CrossRef](#)]
39. Śliwa, T.; Stryczek, S.; Wysogład, T.; Skakuj, A.; Wiśniowski, R.; Sapińska-Śliwa, A.; Bieda, A.; Kowalski, T. Impact of graphite and diatomite on the strength parameters of hardened cement slurries. *Przemysł Chem.* **2017**, *96*, 960–963. [[CrossRef](#)]
40. Kremieniewski, M. Influence of Hblock Fine-Grained Material on Selected Parameters of Cement Slurry. *Energies* **2022**, *15*, 2768. [[CrossRef](#)]
41. Cai, Y.; Hou, P.; Cheng, X.; Du, P.; Ye, Z. The effects of nanoSiO<sub>2</sub> on the properties of fresh and hardened cement-based materials through its dispersion with silica fume. *Constr. Build. Mater.* **2017**, *148*, 770–780. [[CrossRef](#)]
42. Yang, G.; Liu, T.; Zhu, H.; Zhang, Z.; Feng, Y.; Leusheva, E.; Morenov, V. Heat Control Effect of Phase Change Microcapsules upon Cement Slurry Applied to Hydrate-Bearing Sediment. *Energies* **2022**, *15*, 4197. [[CrossRef](#)]
43. Feng, H.; Zhu, P.; Guo, A.; Cheng, Z.; Zhao, X.; Gao, D. Assessment of the mechanical properties and water stability of nano-Al<sub>2</sub>O<sub>3</sub> modified high ductility magnesium potassium phosphate cement-based composites. *Mater. Today Commun.* **2022**, *30*, 103179. [[CrossRef](#)]
44. Liu, H.; Jin, J.; Yu, Y.; Liu, H.; Liu, S.; Shen, J.; Xia, X.; Ji, H. Influence of halloysite nanotube on hydration products and mechanical properties of oil well cement slurries with nano-silica. *Constr. Build. Mater.* **2020**, *247*, 118545. [[CrossRef](#)]
45. Liang, R.; Liu, Q.; Hou, D.; Li, Z.; Sun, G. Flexural strength enhancement of cement paste through monomer incorporation and in situ bond formation. *Cem. Concr. Res.* **2022**, *152*, 106675. [[CrossRef](#)]
46. Huang, Z.; Cao, S.; Yilmac, E. Investigation on the flexural strength, failure pattern and microstructural characteristics of combined fibers reinforced cemented tailings backfill. *Constr. Build. Mater.* **2021**, *300*, 124005. [[CrossRef](#)]
47. Kamasamudram, K.S.; Ashraf, W.; Landis, E.N. Cellulose nanofibrils with and without nanosilica for the performance enhancement of Portland cement systems. *Constr. Build. Mater.* **2021**, *285*, 121547. [[CrossRef](#)]
48. Nassiri, S.; Chen, Z.; Jian, G.; Zhong, T.; Haider, M.M.; Li, H.; Fernandez, C.; Sinclair, M.; Varga, T.; Fifield, L.S.; et al. Comparison of unique effects of two contrasting types of cellulose nanomaterials on setting time, rheology, and compressive strength of cement paste. *Cem. Concr. Compos.* **2021**, *123*, 104201. [[CrossRef](#)]
49. Jain, A.; Gupta, R.; Choudhary, R. Performance of self-compacting concrete comprising granite cutting waste as fine aggregate. *Constr. Build. Mater.* **2019**, *221*, 539–552. [[CrossRef](#)]
50. Chicco, J.; Verdoya, M.; Giuli, G.; Invernizzi, C. Thermophysical properties and mineralogical composition of the Umbria-Marche carbonate succession (central Italy). *Spec. Pap. Geol. Soc. Am.* **2019**, *542*, 59–67. [[CrossRef](#)]
51. Catalog of Górażdże Cement, S.A. *Cement, Kruszywa, Beton*; Górażdże Cement S.A.: Chorula, Poland, 2016.
52. Sunny, J.E.; Varghese, R.A.; Sagar, S.; Sujin, P.J.; Reshma, K. Application of Basalt and its Products in Civil Engineering. *Int. J. Eng. Res. Technol.* **2020**, *9*, 06.
53. Cwojdziański, S.; Jodłowski, S. Plamowe koncentracje bazaltowe Masywu Czeskiego i Dolnego Śląska. *Biul. Inf. Geol.* **1982**, *341*, 201–226.
54. *FOX 50 110 C Instrument Manual, LaserComp—TA Instruments 2002–2016*; LaserComp—TA Instruments: Wakefield, MA, USA, 2016.
55. Renpu, W. Chapter 5—Production Casing and Cementing. In *Advanced Well Completion Engineering*, 3rd ed.; Gulf Professional Publishing: Houston, TX, USA, 2011; pp. 221–294. [[CrossRef](#)]